Emergent Materials (2022) 5:105–132
https://doi.org/10.1007/s42247-022-00376-w

REVIEW

Nanotechnology in food and water security: on-site detection of agricultural pollutants through surface-enhanced Raman spectroscopy

Deniz Yılmaz[1] · Beyza Nur Günaydın[2] · Meral Yüce[1]

Received: 28 December 2021 / Accepted: 24 February 2022 / Published online: 9 March 2022

Abstract
Agricultural pollutants are harmful components threatening human health, wildlife, the environment, and the ecosystem. To avoid their exposure, developing prevention and detection systems with high sensitivity and selectivity is required. Most conventional methods, including molecular and chromatographic techniques, cannot be adopted for outdoor on-site detection even though they can provide sensitive and selective detection. Thus, detection platforms that can provide on-site detection via miniaturized and high throughput systems should be developed. As an alternative method, surface-enhanced Raman scattering (SERS) provides unique information about the substances in the presence of plasmonic nanostructures, and it can be portable with the use of portable detection systems and spectrometers. In this study, on-site detection of agricultural pollutants through SERS is reviewed. Three different types of agricultural pollutants were pointed out. On-site detection of biological pollutants, including bacteria and viruses, is reviewed as the first type of pollutant. As a second type, the detection of pesticides, antibiotics, and additives are focused on as chemical pollutants. The third group includes the detection of microplastics and also nanoparticles from the environment.

Keywords SERS · Agricultural pollutants · Food · Water · Pesticide · Microplastics

1 Introduction

Unsafe food and water are defined as the food or water containing harmful microorganisms, or chemical substances by World Health Organization (WHO). According to them, food and waterborne pollutants could cause more than 200 diseases, including diarrheal diseases, acute respiratory infections, meningitis, and cancer. Around the world, almost 1 in 10 people gets ill, and 420 000 people die each year due to foodborne pollutants, while 829 000 people die due to waterborne pollutants [1, 2]. Thus, not only avoiding these pollutants but also detection is crucial for human health, the ecosystem, and the food industry.

Many methods have been developed for the efficient, sensitive, and selective detection of agricultural pollutants. As shown in Table 1, many different techniques, including molecular methods (polymerase chain reaction (PCR)), immunological methods (enzyme-linked immunoassay (ELISA)), and chromatographic methods (high-performance liquid chromatography (HPLC), mass spectrometry (MS)) are frequently used for the detection of agricultural pollutants [3, 4]. Although most of these methods have high sensitivity and selectivity, they require complex steps, equipment, long sample preparation processes, and trained personnel. They cannot be adapted easily to outdoor detection applications. Thus, the development of rapid, accurate on-site detection systems is crucial, which can decrease agricultural pollutants caused toxicity, illnesses, and deaths with rapid detection from the field.

With the emergence of the nanotechnology idea, nanoparticle-based detection systems have been started to use in many different fields ranging from medicine to food safety and the environment. The use of nanotechnology and nanoparticles (Nps) can provide the advantage of miniaturization with high-throughput analysis with the altered properties of the nanostructures compared with bulk properties.

With the nanotechnology idea, SERS has become a powerful vibrational technique that can give information from

✉ Meral Yüce
meralyuce@sabanciuniv.edu

[1] Sabanci University Nanotechnology Research and Application Center (SUNUM), Istanbul 34956, Turkey

[2] Faculty of Engineering and Natural Sciences, Sabanci University, Tuzla, 34956 Istanbul, Turkey

Table 1 Comparison of methods used for the detection of agricultural pollutants [3, 16]

Technique type	Method	Detected analyte	Advantages	Disadvantages
Cultural		Biological pollutants	• Easy to operate	• Long time • Low sensitivity • Hard to distinguish similarities between different bacteria
Immunological	ELISA	Biological pollutants	• High specificity • Can be automated • A large number of samples can be used	• Complex • Low sensitivity • Narrow detection span • False-negative results • Cross-reactivity • Can require pre-enrichment • Requires trained personnel • Requires labeling of antibodies or antigens
	Lateral flow immunoassay	Biological pollutants	• Low cost • High reliability • Easy to operate • High sensitivity • High specificity	• Requires labeling of antibodies or antigens
	Immunomagnetic separation assay	Biological pollutants	• High efficiency • High specificity	• High cost
	Immunoblot technique	Biological pollutants	• High resolution • High sensitivity	• Complex operation
Metabolic technology	Microcalorimetry	Biological pollutants	• Strong versatility • High applicability	• Long cycle • Weak signal
	ATP bioluminescence	Bacteria	• Fast • Easy • High sensitivity	• Hard to distinguish microbial and non-microbial ATP
	DNA probe	Bacteria	• Fast • Accurate • High specificity	• Markers are hard to dissolve
Nucleic acid-based	PCR	Biological pollutants	• High sensitivity • High specificity • Automated • High reliability	• Error due to the non-target DNA amplification • Difficult to distinguish viable and non-viable cells • Affected by PCR inhibitors • Required DNA purification
	Multiplex PCR	Biological pollutants	• High sensitivity • High specificity • Automated • High reliability • Multiplexed detection	• Error due to the non-target DNA amplification • Crucial to design primers • Difficult to distinguish viable and non-viable cells • Affected by PCR inhibitors
	Real-time PCR	Biological pollutants	• High sensitivity • High specificity • Rapid cycling • Reproducibility • Does not require post-amplification products processing • Real-time monitoring PCR amplification products	• High cost • Difficult for multiplexed detection • Affected by PCR inhibitors • Difficult to distinguish viable and non-viable cells • Requires trained personnel • Cross-contamination risk
	qPCR	Biological pollutants	• High accuracy	• Complex equipment • Expensive fluorescent probes • Photobleaching problem
	Nucleic acid sequence-based amplification	Biological pollutants	• High sensitivity • High specificity • Low cost • Does not require a thermal cycling system • Able to detect viable microorganisms	• Requires viable microorganism • Difficulties in handling RNA
	Loop-mediated isothermal amplification	Biological pollutants	• High sensitivity • High specificity • Low cost • Easy to operate • Does not require a thermal cycling system	• Primer design is complicated • Insufficient to detect unknown or unsequenced targets
	Microarray	Biological pollutants	• High sensitivity • High specificity • High throughput • High efficiency • Multiplex detection • Detection of specific serotypes • Labor-saving	• Difficult to distinguish viable and non-viable cells • High cost due to the gene chip preparation and testing costs • Requires trained personnel • Requires oligonucleotide probes and labeling of target genes

Table 1 (continued)

Technique type	Method	Detected analyte	Advantages	Disadvantages
Biosensor based	Electrochemical	Biological pollutants	• Simple • Good repeatability • A large number of samples can be used • Automated • Label-free detection	• Low specificity • High sample volume is required • Analysis may interfere with detection matrices • Many washing steps • A homogenous sample is required
	Optical	Biological, chemical, physical pollutants	• High sensitivity • Fast • Real-time detection • Label-free detection	• Complex equipment required • High cost
	Piezoelectric biosensors	Biological, chemical, physical pollutants	• Automated • High sensitivity	• Complex equipment required
	Mass-based biosensors	Biological, chemical, physical pollutants	• Cost-effective • Easy to operate • Label-free detection • Real-time detection	• Low specificity • Low sensitivity • Long incubation time with the analyte • Many washing and drying steps
Chromatography based	HPLC	Chemical pollutants	• High measurement accuracy • High sensitivity	• Cannot be applied for on-site detection • Complex equipment required • High cost • Requires trained personnel • Complex sample preparation
	GC–MS	Chemical pollutants	• High measurement accuracy • High sensitivity • High selectivity	• Cannot be applied for on-site detection • Complex equipment required • High cost • Requires trained personnel • Complex sample preparation
	TLC	Chemical pollutants	• High measurement accuracy • High sensitivity • High selectivity	• Requires complex equipment • Requires trained personnel
	FTIR	Physical pollutants	• Fingerprint information	• H_2O interference • Requires sample preparation
	Raman spectroscopy	Biological, chemical, physical pollutants	• Fingerprint information • No interference from the H_2O • Little or no sample preparation • Sharper peaks • The signal can be enhanced (SERS)	• Fluorescence interference • Can cause photodecomposition by heat

ELISA, enzyme-linked immunoassay; *FTIR*, Fourier transform infrared spectroscopy; *GC–MS*, gas chromatography-mass spectrometry; *HPLC*, high-performance liquid chromatography; *PCR*, polymerase chain reaction; *qPCR*, quantitative polymerase chain reaction; *SERS*, surface-enhanced Raman spectroscopy; *TLC*, thin-layer chromatography

the fingerprint of the molecules. It provides high sensitivity, low water interference, short detection time, and does not require complex and long sample preparation steps. The obtained signal can be tailored with changing substrate properties, including size, shape, composition, and surface chemistry [5].

SERS is a good alternative for on-site detection systems, which can be integrated with developed SERS probes and portable Raman spectrometers. For the on-site detection, many different detection platforms or SERS probes were fabricated, such as microfluidic devices, paper-based, and swab-based systems [6–9]. With such systems, sample volume can be decreased, sample handling can be automatized, and the whole system can be turned into a portable device. Many excellent review papers have been published in the literature based on the application of SERS on the detection of agricultural pollutants [10–15].

In this review, the application of SERS on the on-site detection of agricultural pollutants was focused on. Agricultural pollutants were classified into three main groups: biological, chemical, and physical pollutants. Biological pollutants include bacteria and viruses, while chemical pollutants include pesticides, antibiotics, and additives. As physical pollutants, microplastics and nanoparticles were focused due to the increasing importance of their detection from the environment with increased consumption in many industries and products.

2 Mechanisms of SERS

Raman spectroscopy (RS) is named after Sir C. V. Raman discovered the Raman scattering in 1928 [17]. In 1930, he was awarded the Nobel prize in physics for his discovery

of this new type of light scattering. RS is an inelastic scattering that can be used to get information about the unique molecular bond vibrations of a molecule. When a sample is irradiated with incident light, light scatters either elastically or inelastically. Most of the light is elastically scattered with the same frequency as the incident light, which is called Rayleigh scattering.

On the other hand, approximately 1 out of 10^6–10^8 photons are inelastically scattered, called Raman scattering. This inelastic scattering has frequency changes (i.e., Raman shifts) between incident photons and scattered photons, resulting in the energy transfer between photon and molecule. If scattered photons gain energy, it is called anti-Stokes Raman scattering; while if scattered photons lose energy, it is called Stokes Raman scattering.

Obtained Raman spectra are composed of Raman shifts, and each Raman peak at one Raman shift belongs to a specific molecular bond which means obtained spectra give a vibrational fingerprint of the molecule. Although Raman spectroscopy provides a vibrational fingerprint of the molecule, it has a very weak nature because only a very small part of the incident photons is inelastically scattered. Thus, detecting low abundant molecules in complex media is not quite possible without any improvement. With plasmonic nanostructures, enhancement of the Raman signal ranging from 10^7 to 10^{14} can be achieved, and this phenomenon is called surface-enhanced Raman scattering (SERS) [18].

SERS was firstly observed by Fleischmann et al. in 1974 on a roughened silver electrode which increased the Raman signal of pyridine [19]. In 1977, Jeanmaire et al. and Albrecht et al. explained this phenomenon with two separate mechanisms [20, 21]. Today, enhancement mechanisms are still under debate, but these two mechanisms are commonly accepted. Jeanmaire et al. proposed electromagnetic field enhancement (EM) theory, resulting from the surface plasmon polaritons (SPPs). Surface plasmons are the collective oscillation of free electrons in the conduction band of the noble metal. When surface plasmons oscillate with the incoming laser at a frequency, it creates an electromagnetic field gradient formed in a very thin zone (~ 10 nm). When a molecule comes close vicinity to the SERS substrate (plasmonic metal structure), Raman scattering from the molecule is enhanced by the localized electromagnetic field. EM enhancement depends on the resonance between plasmons, excitation, and scattered field. Moreover, when excitation light and Raman scattering are in resonance with the surface plasmon frequency, obtained SERS signal is maximized by a factor (enhancement factor, EF) of about 10^5–10^6 [22].

Albrecht et al. proposed chemical enhancement (CE) theory based on the charge transfer mechanism. When a molecule is adsorbed on a metal surface, chemisorption causes new electronic state formation, mostly called charge transfer state. This newly formed state could serve as resonant intermediate states in Raman scattering and increase the Raman probability of the adsorbate, resulting in enhancement of the Raman signals [23, 24]. If the new charge transfer state is in resonance with the incident light, obtained SERS signal can be maximized by a factor of 10^3 [23].

3 Detection of biological pollutants

When agricultural products are considered, it is not easy to avoid microorganisms. For foods, due to their nutrient composition, they are excellent growth media for microorganisms. On the other hand, water can also contain microorganisms, including bacteria, viruses, fungi, and parasites. As an example of water and foodborne bacteria, *Salmonella typhi*, *Vibrio cholerae*, *Shigella* spp., *Escherichia coli (E. coli)*, and *Yersinia enterocolitica* can be given. Hepatitis A, hepatitis E, norovirus, sapovirus, and rotavirus are examples of pathogenic viruses [25, 26]. These microorganisms could cause infections, illnesses, and severe cases, leading to hospitalization and death [1, 2]. Thus, their detection is crucial to prevent water and foodborne pathogen-related diseases, and SERS is an alternative method that can be used for outdoor detection with portable systems.

Examples of SERS-based on-site detection of biological pollutants are given in Table 2. It includes detailed information about the prepared SERS probes with selected SERS substrates, recognition elements, reporter molecules, detected pollutants, detection matrixes as the real samples, enhancement factor (EF), limit of detection (LOD) of the proposed probe, statistical analysis used for the measured SERS signals, and applicability for the on-site detection.

3.1 Bacteria

Food and waterborne pathogens such as *Salmonella*, *Campylobacter*, and Enterohaemorrhagic *Escherichia coli (E.coli)* can be found in unpasteurized dairy products, raw or undercooked poultry, seafood, tap water, drinking water and can cause fever, headache, nausea, vomiting, abdominal pain, and diarrhea [1, 2]. Although there are many methods based on cultural or immunological techniques for their detection, advancement in on-site detection is crucial. As an on-site detection system, SERS is a widely used powerful technique that can provide rapid, specific, sensitive, and on-site detection [12, 47, 48].

As an example of the on-site detection of bacteria with colloidal nanoparticles-based SERS, Hong et al. [49] compared a total of nine SERS substrates, including commercial 6 AuNPs, 1 AgNPs, and two surfaces as gold and silver for the detection of 6 different bacteria: *E. coli*, *E. coli* O157:H7, *Salmonella* spp., *Listeria monocytogenes*,

Staphylococcus aureus, *Bacillus cereus*, and *Bacillus thuringiensis.* Some of the nanoparticles were stabilized with silica shell coating. Bacterial suspensions were mixed with nanoparticles or added to the surfaces for the measurements. A portable Raman system was used, and this label-free approach showed that among the seven nanoparticles, only two of them provided reproducible signals while surfaces could not provide any repeatable signal. Although two nanoparticles provided reproducible signals, they could not differentiate bacterial strains. Furthermore, EF or LOD of the selected substrates were not calculated. Thus, strains could not be discriminated even from one-bacteria-containing solutions, which means that these commercial substrates require labeling, targeting, or chemometric analysis to develop efficient on-site detection devices to identify bacterial strains**.**

Instead of using commercial SERS substrates, Pan et al. [30] developed a Dual Immunological Raman-Enabled Crosschecking Test (DIRECT) to detect *E. coli* on low moisture foods (LMFs). They have synthesized AuNRs as SERS substrate and then functionalized them with 4-ATP as a Raman reporter molecule. 4-ATP functionalized AuNRs were then modified with *E. coli* antibody as the last step. The developed SERS probe was mixed with spiked black pepper and egg samples for the measurements, and measurements were obtained by a fiber-optical probe integrated with a portable Raman spectrometer. It was claimed that the developed DIRECT system does not require any washing or separation step for the removal of unbound nanoprobes. Because nonspecific bindings could not provide enough SERS signal to create false-positive results. Not only the signal from 4-ATP but also bacteria was used to identify the bacteria, resulting in the detection of 10^2 bacteria in black pepper and egg samples in 30–45 min**.**

To develop a portable detection system, Wang et al. [50] fabricated a nano-dielectrophoretic microfluidic device that detects *E. coli* via SERS, as shown in Fig. 1A. They have constructed SERS probes from gold nanorods (AuNRs) and gold nanocages which are functionalized with 3 different Raman reporter molecules (4-aminothiophenol, 4-ATP; 3-amino-1,2,4-triazole-5-thiol, ATT; and 3-mercaptopropionic acid, 3-MPA) and 3 anti-*E.coli* antibodies targeting different epitopes of the same bacteria. This system monitored dual signals from both Raman reporters functionalized SERS probes and the bacterial target, similar to the previous report. Even though there is a nonspecific binding, it could not provide any dual signals. Thus, only the spectra that include dual signals detected the two *E. coli* strains without any modification, washing, or separation steps. A microfluidic system was integrated to detect two bacterial strains in the same batch, and it provided LOD as 1 $CFU{\cdot}mL^{-1}$. Discrimination and classification of strains were obtained by principal component analysis (PCA) and a binary-based classification algorithm based on a support vector machine (SVM). Used statistical analysis tools confirmed the identification of two strains in a mixture with 95% accuracy. As a consequence, the proposed system provided reduced unspecific binding interference without any washing or separation steps with high LOD value, even though they did not provide any information about the detection from real samples.

As a different microfluidic-based system, Dina et al. [51] reported detection of *E. coli*, *Pseudomonas aeruginosa*, *S. aureus*, and *Enterococcus faecalis* from a microfluidic flow-cell platform coupled with a portable Raman spectrometer. Other from the study of Wang et al., silver spots as Ag nanoclusters were generated inside the microchannel by simultaneous injection of silver nitrate and sodium citrate. Then, bacteria are injected through channels and adsorbed on the substrate due to the affinity of cell wall components to the Ag nanoclusters. Three Raman peaks as marker bands were detected for each species. Although concentration-based information or real sample application were not included in the study, they have claimed that preparation of the Ag clusters inside the microfluidic channels provided stability to the nanoparticles.

As a more recent example with surfaces instead of nanoparticles, deterministic aperiodic gold nanocavities were fabricated using electron beam lithography (EBL) to detect *Brucella abortus* in milk, shown in Fig. 1B [27]. They have used 4-aminothiophenol (4-ATP) as Raman reporter and Tbilisi bacteriophages as a recognition element that captures the bacteria. As a more comprehensive study, they have calculated the EF value as 3.8×10^6 using 4-mercaptobenzoic acid (4-MBA). But there was not any EF calculation for the surfaces functionalized with 4-ATP. Bacteria spiked water and milk samples were dropped on the surface for the measurements. It was realized that a new peak attributed to the vibrational stretching of the diazo bond (1-ATP-N = N-Tb) is observed with the captured *Brucella.* With the use of this peak, ~ 10^4 viable bacterial cells were identified in the spiked milk samples.

3.2 Viruses

Norovirus, rotavirus, astrovirus, and hepatitis A are among the most common viral pathogens that can be found in raw or undercooked food and water. They can cause gastroenteritis, nausea, diarrhea, vomiting, and cramps [1, 2, 52, 53]. Moreover, the avian influenza virus is among the most studied viruses for detection via SERS due to the caused big losses in the poultry industry. Sun et al. [38] reported avian influenza virus H3N2 detection with a portable magnetic SERS immunosensor. They used AuNPs as SERS substrate, 4-MBA as Raman reporter, and influenza IgG as a recognition element. As a first step, they have prepared a common

SERS substrate combination which consists of a metal nanoparticle core and modified surface with reporter molecule and recognition element. But then, they have synthesized Fe_3O_4 Nps, which were adsorbed onto the AuNPs surface using inositol hexakisphosphate as a bridge. To prepare a sandwich assay, they have conjugated the Fe_3O_4/AuNPs with an antibody. They have mixed antibody-labeled 4-MBA-AuNPs and antibody-labeled Fe_3O_4/AuNPs to sandwich the virus between them, which increased the sensitivity. They tracked the dominated peaks of 4-MBA and detected the virus down to 10^2 tissue culture infection doses at 50% endpoint (TCID)·mL^{-1} when a portable Raman spectrometer was used. There were no real sample trials, but they have concluded that the developed system can be used for the real samples for on-site virus infection diagnosis with a portable Raman spectrometer.

Different from the sandwich assay, Xiao et al. [7] utilized a lateral flow immunoassay (LFA) strip-based system for the detection of avian influenza A (H7N9) via SERS, as shown in Fig. 2A. They used silver-coated colloidal gold core–shell Nps as SERS substrate. Core–shell Nps were functionalized with 4-ATP as Raman reporter, and EF was calculated as 3.5×10^6. The probe was then coated with polyvinylpyrrolidone (PVP) for protection and covered with AgNPs. As the last modification, the H7N9 antibody was conjugated as a recognition element on the surface. For the fabrication of lateral flow assay, they have used a sample pad, adsorbent pad, conjugation pad, nitrocellulose (NC) membrane, and plastic backing. The SERS probe was dispensed onto the conjugation pad; H7N9 antibody and anti-IgG antibody were dispensed to the test and control line on the NC membrane as capturing element and negative control, respectively. All parts were assembled, cut into strip shape, and fit into a plastic housing. When the virus bound to the SERS probe, it formed an immunocomplex that migrates along the NC membrane by capillary action. When it reached the test line, it was captured by capture antibody immobilized on the test line and capturing observed by the naked eye. In the control line, only SERS nanoprobes were captured by the IgG antibody, which can also be seen by the naked eye. Thus, in the presence of the virus, two bands were observed by the naked eye, whereas only one line, including only probes, can be seen in the absence of the virus. The virus was quantified using a portable Raman spectrometer and detected in 20 min with 0.00118 hemagglutinating unit (HAU), three orders of magnitude more sensitive than conventional hemagglutination assay (HA). They also used 20 H7N9 samples from different organs of poultry. They first spiked different amounts of virus to the avian cloaca and obtained the LOD as 0.0035 HAU. As an important observation, they have also used real cloacal and throat swab samples of poultry without spiking the analyte and compared the SERS results with the real-time polymerase chain reaction (RT-PCR) as a reference method. They have obtained comparable, consistent, and reproducible SERS results from the samples with a similar accuracy of RT-PCR. This study showed that detection from developed LFA strips is easier than performing RT-PCR, and it does not require trained personnel and sample purification.

Another pandemic virus, Severe Acute Respiratory Syndrome Coronavirus 2 (SARS-CoV-2) was also focused on detecting, but there are few on-site detection applications with SERS. Zhang et al. [36] detected SARS-CoV-2 in water via SERS using cellular receptor angiotensin-converting enzyme 2 (ACE2) receptor functionalized AgNRs array. They showed that binding of the receptor-binding domain (RBD) of SARS-CoV-2 spike protein to the ACE2 receptor caused a reduction in the band intensities and a significant shift. They used 23 water samples from rivers, hospitals, and pipe networks for on-site detection using a portable Raman spectrometer. The RNA content of the real samples was identified with real-time reverse transcription-quantitative polymerase chain reaction (RT-qPCR) without spiking. RT-qPCR results classified the water samples into negative and positive for the presence of SARS-CoV-2. When obtained results were compared with the SERS results, SERS provided significant discrimination of negative and positive groups with an accuracy of 93.33%. Consequently, the proposed detection method provided accurate on-site detection of the virus in the real samples in real conditions, as shown in Fig. 2B.

Other foodborne and waterborne viruses are also detected by SERS using portable systems. Yadav et al. [37] fabricated Ag nanoarrays for the on-site detection of the human immunodeficiency virus (HIV-1) in water samples, as shown in Fig. 2C. The angle deposition method was used for synthesis, and the synthesized array provided EF as 2.3×10^9. Without any further modification, viruses directly bound to the AgNRs. They have spiked the water samples with 5 different subtypes of HIV-1 and showed that two subtypes of the virus provided differences in obtained SERS spectra. Detectable amounts of the virus were found in between 10^2 to 10^5 copies·mL^{-1} with a portable Raman spectrometer. Although they did not provide any results from real samples without spiking, they have claimed that the proposed study shows the potential of SERS to detect and differentiate viruses from clinical samples and isolates.

4 Detection of chemical pollutants

In agriculture, many different chemicals are used not only to protect the produced crops but also to increase the production rate and change the properties of the food.

Table 2 SERS-based detection of biological pollutants from food and water

Category of the pollutant	Pollutant	SERS substrate	Synthesis of the SERS substrate	Recognition element	Raman reporter molecule	Total SERS probe	Detection matrix	EF	LOD	Detection time	Data analysis	On-site detection	Ref
Bacteria	*Brucella abortus*	Au layer	EBL	Tbilisi bacteriophages via diazo coupling	-	Deterministic aperiodic nanocavity patterned gold nanoarray	Spiked water and milk	3.8×10^{6}	10^{4} viable cells	-	-	+	[27]
Bacteria	*E. coli*	AgNPs	Purchased	-	-	AgNPs patterned paper	PBS	-	10^{5} CFU	-	-	+	[28]
Bacteria	*E. coli DH5α, Pseudomonas taiwanensis*	AgNPs	Lee–Meisel protocol	-	-	Microfluidic device with an incorporated nanoporous membrane	Spiked drinking tap water	-	-	-	-	+	[6]
Bacteria	*Staphylococcus aureus* biofilm	AuNPs	Chemical reduction method	CV	CV	-	-	-	-	17 min	PCC	+	[29]
Bacteria	Non-pathogenic *E. coli*	AuNRs	Seed-mediated growth method	Anti-*E. coli* antibody	4-ATP	*E. coli* antibody@4-ATP@ AuNRs	Spiked black pepper, egg powder	-	10^{2} CFU·g^{-1}	30–45 min	PCA-SVM	+	[30]
Bacteria	*E. coli O157:H7*	AuNPs	Sodium citrate reduction method	Anti-*E. coli* O157:H7 antibody	Homonucleotides consist of adenine or thymine	Homonucleotide-embedded Au@Au core–shell nanoparticles	Spiked fruit juice samples	-	2 CFU·mL^{-1}	-	-	-	[31]
Bacteria	*Y. pestis, F. tularensis, B. anthracis*	AuNPs	Seed-mediated growth method	Anti-*Y. pestis,* Anti-*F. tularensis*, and Anti-*B. anthracis* antibodies	MGITC	LFA strips	Buffer solution	-	*Y. pestis:* 43.4, *F. tularensis:* 45.8, *B. anthracis:* 357 CFU·mL^{-1}	15 min	-	-	[32]
Bacteria	*A. baylyi*, *E. coli*	Silver-coated MNPs	Chemical co-precipitation coating: glucose reduction	-	-	Silver-coated MNPs	Drinking water	10^{3}	10^{5} CFU·mL^{-1}	< 15 min	-	-	[33]
Bacteria	*C. parvum*, *E. coli*, *Staphylococcus aureus*	AgNPs	Lee and Meisel method	-	-	AgNPs	Distilled water	-	-	-	PCA HCA	-	[34]

Table 2 (continued)

Category of the pollutant	Pollutant	SERS substrate	Synthesis of the SERS substrate	Recognition element	Raman reporter molecule	Total SERS probe	Detection matrix	EF	LOD	Detection time	Data analysis	On-site detection	Ref
Virus	Hepatitis A virus	Au nanopyramids	EBL	Anti-hepatitis A virus antibody	-	Inversed pyramidal nanoholes array	Water	6×10^6	68 pg·ml^{-1}	-	-	-	[35]
Virus	SARS-CoV-2	AgNRs array	Electron beam/sputtering evaporation system	ACE2	-	ACE2@AgNRs array	Waters collected from rivers, hospitals, and pipe networks in Wuhan	-	-	2 min	PCA-LDA	+	[36]
Virus	HIV	AgNRs array	Electron beam evaporation	-	-	AgNRs array	Spiked diethylpyrocarbonate treated water	2.3×10^9	-	-	PCA	+	[37]
Virus	Avian influenza A	Au@AgNPs	Sodium citrate reduction method	Anti-H7N9 antibody	4-ATP	LFA strip	Different organs of poultry	3.5×10^6	0.0018 HA	20 min	-	+	[7]
Virus	Avian influenza virus (H3N2)	AuNPs	Frens' method	Anti-Influenza A antibody	4-MBA	Fe_3O_4/Au NPs@4-MBA@ Influenza A antibody	Real sample for on-site virus infection diagnosis	-	10^2 $TCID_{50}$·mL^{-1}	-	-	+	[38]
Virus	SARS-CoV-2	AgNPs	Qin's method	Anti-SARS-CoV-2 spike antibody	4-MBA	AgNPS@4MBA. SARS-CoV-2 spike antibody modified SERS	Untreated saliva	-	6.07 fg·mL^{-1}	-	-	-	[39]
Virus	SARS-CoV-2	AuNSs	Seed-mediated growth method	Anti-SARS-CoV-2 nucleocapsid antibody	MGITC	Sandwich assay between SERS nanotags and magnetic beads	Clinical sample	-	5.1 PFU·ml^{-1}	-	-	-	[40]
Virus	SARS-CoV-2	AgNPs	Wet chemical deposition	-	-	SiNWs/AgNPs sensor	PBS	-	9.3 pM 2.4 pg·μL^{-1}	<5 min	-	-	[41]
Antibodies against SARS-CoV-2	SARS-CoV-2 IgM/IgG	Silver-coated AuNPs	Sodium borohydride reduction method	SARS-CoV-2 IgM/IgG antibody	DTNB	Dual-layers DTNB-modified SiO_2@Ag NPs@AuNPs based LFA	Human serum	-	1 pg·mL^{-1}	-	The receiver operating characteristic curve analysis	+	[42]

Table 2 (continued)

Category of the pollutant	Pollutant	SERS substrate	Synthesis of the SERS substrate	Recognition element	Raman reporter molecule	Total SERS probe	Detection matrix	EF	LOD	Detection time	Data analysis	On-site detection	Ref
Antibodies against Norovirus	Norovirus (NoV)	AgNCs	Purchased	Anti-NoV antibody	Polydopamine-functionalized MNPs	Anti-NoV-S-agCDs @ poly(dop)-MNPs-AgNCs	10% human serum	10^8	6.5 fg·mL^{-1}	-	-	-	[43]
Parasite	*G. lamblia* cysts	AuNPs	Sodium citrate reduction method	Anti-*Giardia* antibodies	RBITC	Immunogold conjugated membrane filters	Drinking water	-	-	-	-	-	[44]
Parasite	*Entamoeba histolytica*	AuNPs	Seed-mediated growth method	Nanoyeast single-chain variable fragments (NYscFv)	MNBA and 4-MBA	Duplex microfluidic silica-coated AuNP utilizing NYscFv	PBS	-	1 pg·mL^{-1}	-	-	-	[45]
Parasite	*C. parvum* oocysts and *G. lamblia*	AuNPs	Frens' method	Anti-*C. parvum* and Anti-*G. lamblia* antibodies	RBITC, FITC, MGITC, XRITC	Immunogold conjugates with antibodies and four fluorescent dye molecules	PBS	-	-	-	-	-	[46]

4-ATP, 4-aminothiophenol; *4-MBA*, 4-mercaptobenzoic acid; *ACE2*, angiotensin-converting enzyme 2; *AgNCs*, silver nanocubes; *AgNPs*, silver nanoparticles; *AuNPs*, gold nanoparticles; *AuNRs*, gold nanorods; AuNSs, gold nanostars; *CFU*, colony-forming unit; *CV*, crystal violet; *DTNB*, 5,5-dithiobis-(2-nitrobenzoic acid); *EBL*, electron beam lithography; *EF*, enhancement factor; *FITC*, fluorescein isothiocyanate; *HAuCl4*, chloroauric acid; *HCA*, hierarchical cluster analysis; *HIV*, human immunodeficiency virus; *LDA*, linear discriminant analysis; *LFA*, lateral flow assay; *LOD*, limit of detection; *MGITC*, malachite green isothiocyanate; *MNBA*, 4-mercapto-3-nitro benzoic acid; *MNPs*, magnetic nanoparticles; *PCA*, principal component analysis; *PCC*, Pearson correlation coefficient; *PBS*, phosphate-buffered saline; *RBITC*, rhodamine B isothiocyanate; *SERS*, surface-enhanced Raman scattering; $TCID_{50}$, tissue culture infection dose at 50% endpoint; *XRITC*, x-rhodamine isothiocyanate

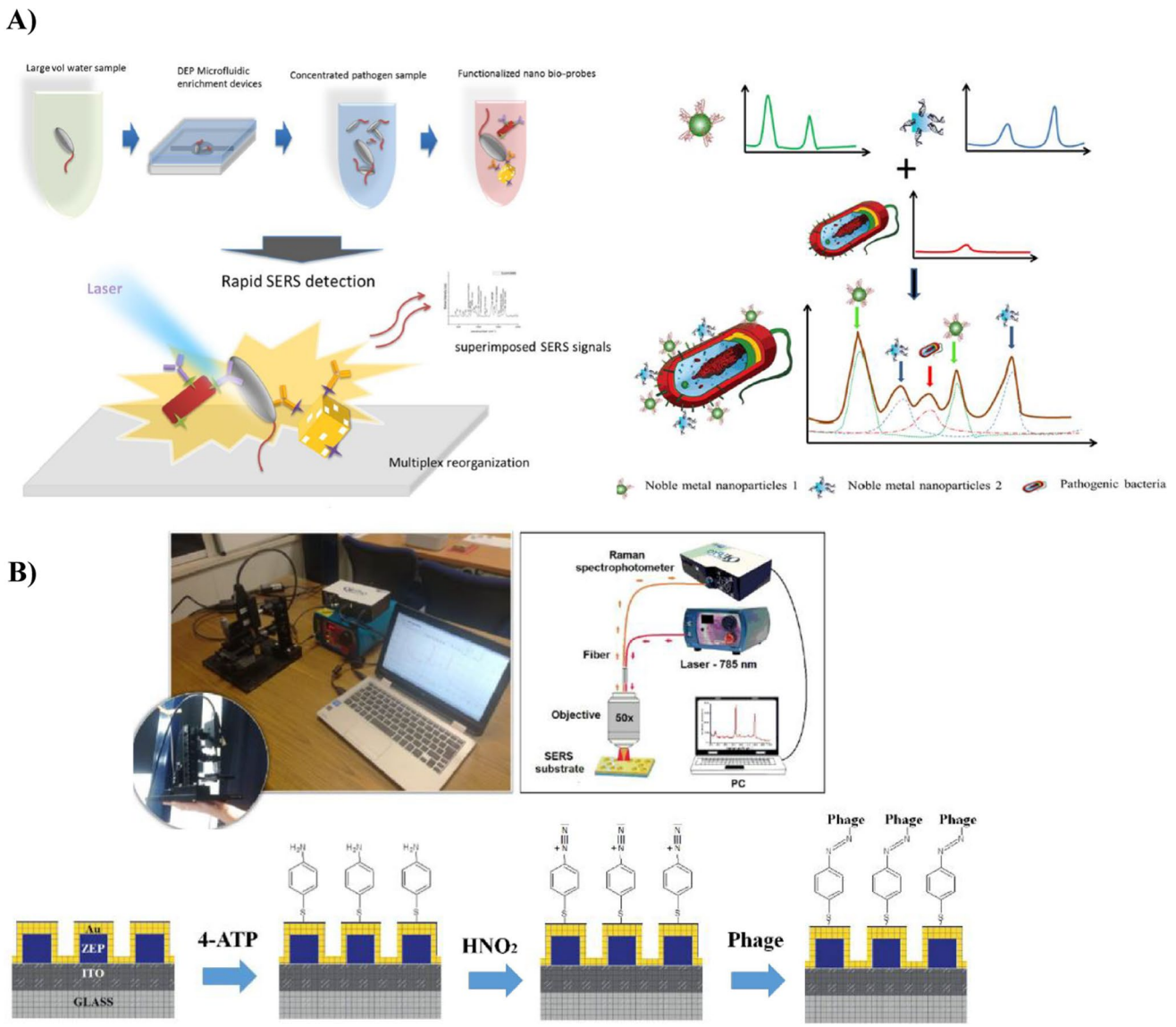

Fig. 1 SERS-based on-site detection of bacteria. **A** SERS-based detection of *E. coli* with a developed nano-dielectrophoretic microfluidic device. Reproduced with permission from Ref. [50]. B Fabrication of deterministic aperiodic gold nanocavities using electron beam lithography (EBL) for the detection of *Brucella abortus* in milk. Reproduced from Ref. [27]

Chemical pollutants include pesticides used for the protection of crops, antibiotics used for the control of diseases, additives, and dyes used to alter the properties of the food, heavy metals from the environmental and anthropogenic activities, and small molecules caused by natural and industrial activities [1, 2, 54, 55]. To detect different types of chemical pollutants, SERS is also used with the potential of on-site detection (Table 3).

4.1 Pesticides

More than 1000 pesticides around the world are used for the protection of crops against insects, weeds, fungi, and other types of pests. They are essential in modern agriculture, which increases farm productivity [82]. Due to their toxicity-based mechanism of action and ability to remain on the foods as well as in soil and water for long times, they create risks to human health, wildlife, and the environment [55]. Exposure to pesticides can cause acute and chronic diseases, which lead to 3,000,000 poisonings and 220,000 death each year, according to the WHO [83]. Thus, detection of pesticide residues is crucial, and SERS has been extensively used for the detection of pesticide residues not only in the solutions but also from real samples [84]. Here, we focused on the on-site detection of pesticides with portable systems.

As an example of a colloid-based detection study, Xu et al. developed popcorn-like AuNPs for the on-site detection of chlorpyrifos (CPF) on the pear samples [67]. They have prepared the AuNPs with the seed-mediated growth method, which includes reduction of chloroauric acid with ascorbic acid as seed, then growing the formed seeds with hydroxylamine hydrochloride. Then, they prepared pear samples as spiking CPF onto the pear peels. The sample was dried, crushed in acetonitrile, centrifuged, and obtained supernatant was mixed with Au nanopopcorns for the SERS measurements. Synthesized popcorn structures provided 1.8×10^5 enhancement of the Raman signal where the LOD was found as 0.35 mg·kg^{-1} for pear samples. They have also confirmed the SERS results with HPLC–MS for the spiked pear samples and found that SERS provided similar recovery rates with HPLC as 84.5 to 95.83% for SERS and 93.5 to 100.83% for HPLC. Although they did not provide any information about real sample applications without any spiking, they have shown that SERS can provide detection of pesticides with similar recovery rates compared with a highly sensitive HPLC–MS method.

Instead of working on one pesticide on real samples, Dowgiallo et al. [85] provided bare colloidal AuNPs based detection of 21 pesticides (neonicotinoid pesticides, organothiophosphate insecticides, fungicides, and insecticides) via SERS. They have directly mixed the bare 45-nm AuNPs with different amounts of pesticides. For the real sample detection, pesticide solutions were spiked on the apple skin, and apple skin was mixed with AuNPs before the measurement. The detection range was between 0.001 and 10 ppm. As a different and crucial investigation, they have also tried to distinguish two pesticides in the same solution. Phosmet and thiram were selected due to their strong and characteristic Raman signal. Different volume ratios of the pesticides were used for the observation of discrimination. Two distinct bands were chosen to compare pesticides and tracked in solutions and apple skin samples. Using PCA as a multivariate analysis method, the separation of two pesticides was achieved based on their concentration ratio in solution and apple skin samples. Their results showed that SERS could be used for the simultaneous on-site detection of pesticides with high sensitivity and selectivity, even using only bare nanoparticles without further modifications.

For the extraction of pesticides from foods, Chen et al. [8] used an AuNPs dropped tape to extract the pesticides from the fruit skins, as shown in Fig. 3A. They first dropped 25 nm AuNPs on the tape, called SERS-tape, then pasted it on the apple, orange, cucumber, and green vegetables where parathion-methyl, thiram, and chlorpyrifos was sprayed on the cleaned peels of foods. Before the measurement, the tape was removed from the sample surface and used for the SERS analysis with a portable Raman spectrometer. They compared commercial adhesive tapes for their sticky feature to extract pesticide and interference with the SERS signal. Out of the five commercial tapes, they selected "3 M transparent adhesive tape" with a higher SERS signal and more negligible background fluorescence noise. The developed substrate provided 1.3×10^5 EF. For the real samples, they have observed major characteristic peaks of pesticides, which provided detection limit of parathion-methyl up to 2.60 ng·cm^{-2}, thiram up to 0.24 ng·cm^{-2}, and chlorpyrifos up to 3.51 ng·cm^{-2} from the peel samples. They have compared their results with the previous work published in 2012 [86] and said that their tape yielded better LOD and high sampling efficiency, even they did not calculate the extraction efficiency.

Similar to Chen et al., Gong et al. [59] also used tape-based extraction of the pesticides while they extracted the pesticides with tape and then added AgNPs onto the tape for SERS measurements. Similar to the previous group, they have checked 3 different commercial adhesive tapes and compared their efficiency using R6G on the aluminum foil. They found that "3 M Post-it" adhesive tape provided higher signals of R6G without any background interference. They did not calculate the EF, but sample collection efficiency from glass surface was calculated as 60.2%. In comparison, it was 54.3% for the aluminum foil due to its roughness. For the real samples, similar to Chen et al., they have spiked the triazophos on the apple and cherry tomatoes peels. Differently, they have pasted the tape on the samples, and then AgNPs were added onto the tape. Measurements were obtained in a wet state via a portable Raman spectrometer. Sample collection efficiency was calculated as 52% and LOD as 2.5 ppmv (25 ng·cm^{-2}) for triazophos on apple peels. When two similar methods were compared, it can be said that the addition of the nanomaterial before the extraction of pesticide provided a tenfold better LOD value for the detection from peel samples.

Jiang et al. [87] used a nanoarray instead of colloidal SERS substrates for pesticide detection and commercial tapes to extract pesticides, similar to the previous reports. Al_2O_3-coated AgNRs array was fabricated via oblique angle deposition method using an electron beam system. Al_2O_3 layer was used for the protection of silver being oxidized. SERS measurements were obtained by a portable micro-Raman spectrometer. They checked the intensity change when a tape is wrapped on the array using 4-mercaptopyridine (4-MPY) and found that the signal of 4-MPY reduced by 1.61 times after wrapping, which was thought as negligible. They have also tried the system by extracting 4-MPY from a glass slide using tape and showed that a clear signal could be obtained from 4-MPY. R6G was used to determine extraction efficiency, and it was found as 91.6%. As a pesticide detection application, tetramethylthiuram disulfide (TMTD) and thiabendazole (TBZ) were detected from apple, pear, cucumber, and spinach samples. Peels were washed,

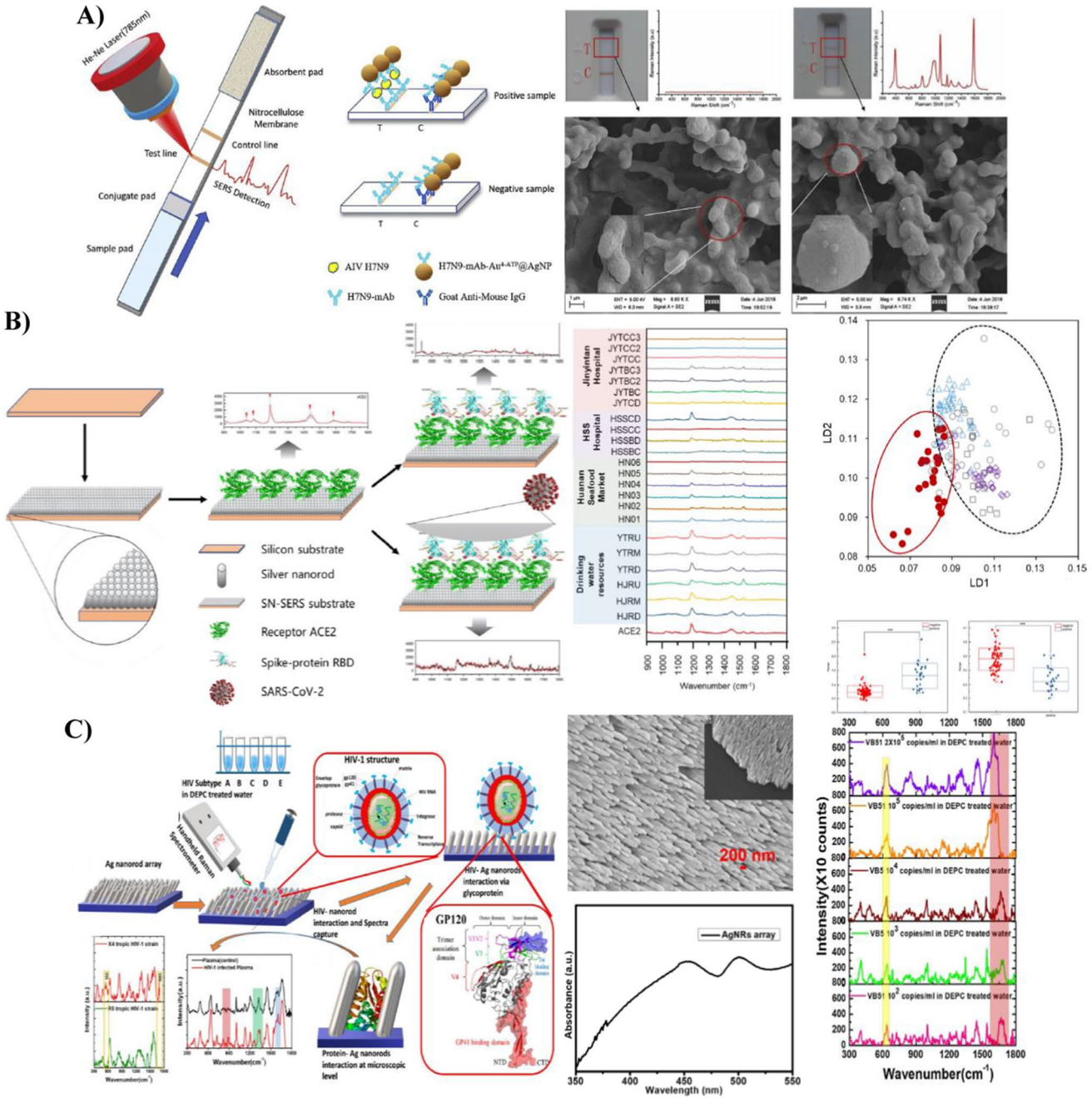

Fig. 2 SERS-based on-site detection of viruses. **A** Fabrication of a lateral flow immunoassay strip-based SERS detection of avian influenza A using core–shell Au–Ag nanostructures. Reproduced with permission from Ref. [7]. Copyright 2019 Elsevier. **B** Detection of Severe Acute Respiratory Syndrome Coronavirus 2 (SARS-CoV-2) in water by angiotensin-converting enzyme 2 (ACE2) receptor functionalized AgNRs array. Reproduced with permission from Ref. [36]. Copyright 2021 Elsevier. **C** On-site human immunodeficiency virus (HIV-1) detection in water via Ag nanoarrays. Reproduced with permission from Ref. [37]. Copyright 2021 Elsevier

cut into desired sizes, sprayed with pesticide solutions, and dried naturally. Then, the tape was used for the extraction and then pasted onto the arrays, as shown in Fig. 3B. Bands of the pesticides from each sample were observed clearly. Although the detection limit for apple peels was calculated as 10 μM (28.8 ng·cm^{-2}) for TMTD, the LOD values for other types of pesticides and samples were not provided.

Flexible, robust, and reproducible SERS substrate was developed by another group [57] for the on-site detection of thiram and parathion-methyl on apple. They designed

4-ATP covered AuNPs/PVC film and detected thiram and parathion-methyl on the apple by wrapping it around the apple and tracking the Raman signal of the 4-ATP. They detected thiram with a 10 $ng{\cdot}cm^{-2}$ concentration limit. The flexible structure provided easy measurement without any sample extraction or sample preparation from the real samples. Still, it could not achieve the LOD value that Chen et al. [8] showed, who calculated LOD as 2.60–3.51 $ng{\cdot}cm^{-2}$ with the developed SERS-tape method.

As a different study, Guselnikov et al. [88] used metal–organic framework (MOF)-coated gold gratings. The gold grating was fabricated by depositing a gold thin film onto a patterned polymer surface using excimer laser patterning, and it was modified with diazonium as a linker for MOF coating. MOF structure was used for entrapping pesticides with the adsorption ability. The EF of the fabricated grating was calculated as 10^6. Paraxon-ethyl and fenitrothion pesticides were detected at a concentration as low as 10^{-12} M (2.8×10^{-7} $mg{\cdot}L^{-1}$) in solutions. When they used soil as an environmental sample, sequential extraction was applied with solvents such as water, acetonitrile, ethanol, and chloroform. The recovery rate and LOD were calculated as 97.5% and 10^{-10} M, respectively. Different from the previous studies, they have used soil as a more complex matrix and showed that SERS could detect pesticides from that complex matrix in a nanomolar range.

4.2 Antibiotics

Antibiotics are essential to treat infections caused by bacteria. However, their over- and misuse in veterinary and human medicine has been linked to the emergence and spread of resistant bacteria, rendering the treatment of infectious diseases ineffective in animals and humans. Besides, antibiotics can be directly used on food to alter the shelf-life properties, or resistant bacteria can also enter the food chain through the animals (e.g., *Salmonella* through chickens) [1, 2]. Thus, understanding the antibiotic content of the food is crucial, and SERS can be used for the on-site detection of antibiotics.

As an example of antibiotic detection by SERS, Wu et al. [89] used raspberry-like Au nanostructures for the on-site detection of antibiotics in duck meats. Nanostructures were synthesized by seed growth of Ag particles, then substitution by Au particles via replacement reaction. EF of the designed nanostructures was calculated as 10^6 using violet (CV) and malachite green (MG). Then, antibiotic drugs nitrofurantoin (NFT) and nitrofurazone (NFZ) were detected in spiked duck meats by mixing mashed duck meat and antibiotics, then extracting the antibiotics using hexane, dichloromethane, and acetone. After extraction, samples were mixed with the nanostructures for measurement. The least amount they could detect was 0.05 $mg{\cdot}L^{-1}$ for NFZ and NFT, where the recovery rate was ranged from 98.1 to 105.6% for NFT and 97.9–108.5% for NFZ from the duck meat samples.

As another example of colloidal nanoparticle-based SERS, Fa et al. [68] green-synthesized AgNPs to detect oxytetracycline (OTC) in honey samples. AgNPs, potassium carbonate, honey, and antibiotics were mixed and centrifuged. Then, the second centrifugation was done with the addition of fresh AgNPs and NaOH onto the centrifuged solution to obtain an in situ synthesis of AgNPs with the reducing sugars of the honey. This second synthesis was used to adsorb the remaining OTC after the first centrifuge. A concentration range between 5 and 20 ppb of OTC was detected by SERS. Moreover, they also investigated the interaction between OTC^{2-} and Ag clusters, where interaction was found through the oxygen and/or nitrogen atoms. Consequently, they have shown that the proposed system could detect antibiotics at the ppb levels with the use of a portable Raman spectrometer,

Shi et al. [90] prepared a more complex detection system for neomycin (NEO) and quinolones (QNS) detection. They have used LFA-based SERS detection where synthesized 40 nm AuNPs modified with 4-ATP and neomycin or norfloxacin (NOR) antibody, which can react with 13 quinolones. The proposed LFA system is composed of a sample application pad, conjugation pad, nitrocellulose membrane, absorption pad, and a backing card similar to other LFA systems. Two test lines with one control line were formed at the center of the nitrocellulose membrane. Ovalbumin bonded NEO and NOR were immobilized to two test lines, and IgG antibody was immobilized to the control line. When there were enough NEO and QNS antibiotics in the sample, they reacted with the antibody-coated AuNPs, which blocked the reaction between the antibodies on the AuNPs with the ovalbumin bonded NEO and NOR on the assay. Thus, no line will be seen when there are antibiotics due to the absence of AuNPs in the test line. The control line would always be visible with the interaction of IgG with NEO and NOR antibodies. With the developed reverse method, which is based on the removal of the line in the strip instead of formation, LOD of the NEO was found as 0.37 $pg{\cdot}mL^{-1}$, and NOR was found as 0.55 $pg{\cdot}mL^{-1}$. When they assessed the specificity of the developed SERS-LFA system, they showed that it could detect NEO and 8 QNS simultaneously. When they used milk as a real sample, an 86% to 121% recovery rate was achieved, which shows that the developed portable system can provide multiplexed detection of antibiotics from a real system with high sensitivity.

4.3 Additives

Among the illegal food additives, many different chemical compounds can be counted. Dyes are frequently used to change the color of the produced food, adulterants, and

Table 3 SERS-based detection of chemical pollutants from food and water

Category of the pollutant	Pollutant	SERS substrate	Synthesis of the SERS substrate	Recognition element	Raman reporter molecule	Total SERS probe	Sample	EF	LOD	Detection time	Data analysis	On-site detection	Ref
Pesticide	TBZ, Thiram	AgNPs	Hydroxylamine reduction method	-	-	Ag colloid immersed cotton swab	Spiked bitter gourd	-	1 $ng{\cdot}cm^{-2}$	-	MLR, PCA	+	[56]
Pesticide	Thiram	AuNPs	Sodium citrate reduction method	-	-	AuNPs/PVC film	Spiked apple	3.7×10^{6}	10 $ng.cm^{-2}$	-	-	+	[57]
Pesticide	Thiram, TBZ	AgNPs	N. Leopold's method	-	-	AgNPs/NC paper-based SERS	Spiked apples and cabbages	-	Thiram: 0.5 $ng{\cdot}cm^{-2}$, TBZ: 5 $ng{\cdot}cm^{-2}$	-	-	+	[58]
Pesticide	Triazophos	AgNPs	Hydroxylamine reduction method	-	-	AgNPs based SERS	Spiked apples and cherry tomatoes	-	25 $ng{\cdot}cm^{-2}$	5 min	-	+	[59]
Pesticide	Phosmet, TBZ, thiram	AuNPs	Sodium citrate reduction method	-	-	Au@SiO_2 core–shell NPs	Spiked apple	-	0.5 $mg{\cdot}kg^{-1}$ for phosmet	-	-	+	[60]
Pesticide	Thiram, tricyclazole, carbaryl	AuNRs	Seed-mediated growth method	-	-	AuNRs-nanoporous cellulose nanofiber	Spiked apple	1.4×10^{7}	Thiram: 6 $ng.cm^{-2}$, tricyclazole: 60 $ng{\cdot}cm^{-2}$, carbaryl: 600 $ng{\cdot}cm^{-2}$	-	-	+	[61]
Pesticide	Dimethoate	AgNPs	Lee-Meisel method	-	-		Olive leaves	10^{3}	5×10^{-7} M		-	+	[62]
Pesticide	Thiram	Au coated Au@Ag nanocubes (NCs)	Seed-mediated growth method	-	-	Au@Ag@Au-NCs/PVC film	secondary effluent from the local wastewater treatment plant, and estuary water from Xinglin Bay	1.1×10^{6}	0.1 ppb	-	-	+	[63]

Table 3 (continued)

Category of the pollutant	Pollutant	SERS substrate	Synthesis of the SERS substrate	Recognition element	Raman reporter molecule	Total SERS probe	Sample	EF	LOD	Detection time	Data analysis	On-site detection	Ref
Pesticide	Thiram, melamine	AgNPs	Purchased	-	-	AgNPs based microelectrodes	Spiked apple juice, milk, and infant formula	5.9×10^5	Thiram: 115 ppb o in apple juice, 1.5 ppm in milk Melamine: 105 ppb in infant formula	<45 min	-	-	[64]
Pesticide	TBZ	AuNPs	Frens' method	-	-	AuNPs on an ultrafiltration membrane	Spiked orange peel	-	0.125 $\mu g \cdot g^{-1}$	-	PLS	+	[65]
Pesticide	Thiram	AgNPs	Leopold and Lendl' method	-	-	AgNPs coated wiper-type filter paper	Spiked apple, pear, and grape	-	4.6 $ng \cdot cm^{-2}$ for apple, 5.1 for pear, 5.7 $ng \cdot cm^{-2}$ for grape peel	-	-	+	[66]
Pesticide	CPF	Popcorn-like AuNPs	Seed-mediated growth method	-	-	Au nanopopcorn	Spiked pear	1.8×10^5	0.35 $mg \cdot kg^{-1}$	-	-	+	[67]
Antibiotics	OTC	AgNPs	D-glucose reduction method	-	-	AgNPs	Spiked honey	-	5 ppb	-	-	+	[68]
Antibiotics	CIP	AuNPs	Sodium citrate reduction method	-	-	Au–Ag heterostructured cubes	Spiked chicken wings		2×10^{-7} M	-	-	+	[69]
Antibiotics	OHC, AT, TH	AgNPs	Seed-mediated growth method	-	-	Ag NPs/CNT-intercalated GO laminar membranes	-	7.2×10^6	OHC: 7.6×10^{-10} M, AT: 3.2×10^{-9} M, TH: 1.5×10^{-9} M	-	-	+	[69]
Additive antibiotics dye	Enrofloxacin, melamine, MG, thiram	AgNPs	Printed	-	-	Printed AgNPs on a glass slide	Milk powder in infant formulation	-	10 ppm for melamine	-	-	+	[70]
Antibiotics	SMM, SD, SDD	β-CD modified AgNPs	In situ reduction method	-	-	β-CD-AgNPs encapsulated PVA hydrogel	Ultrapure water	1.97×10^6	10 $ng \cdot mL^{-1}$	-	-	+	[71]

Table 3 (continued)

Category of the pollutant	Pollutant	SERS substrate	Synthesis of the SERS substrate	Recognition element	Raman reporter molecule	Total SERS probe	Sample	EF	LOD	Detection time	Data analysis	On-site detection	Ref
PAH	Bap	AgNRs array	E-beam evaporation	-	-	AgNRs array	Spiked river water and soil	-	1 ppm in river water, 10 ppm in soil	20 min	Density functional theory	+	[72]
PCB	Bap, PCB	AuNPs	Sodium citrate reduction and a seed-mediated growth method	-	-	Amphiphilic block copolymer-tethered AuNPs with polystyrene-b-poly (ethylene) oxide vesicles	Spiked water and soil	1.87×10^{8}	10^{-12} g·mL^{-1} for Bap and PCB	-	-	+	[73]
Additives	Thiram MG CV	AgNPs	Sodium citrate reduction method	-	-	AgNPs-embedded nylon filter membrane	Spiked soil and apple	-	10 pmol for CV and MG	-	-	+	[74]
Additives	Nucleic acid	AuNPs	Sodium citrate reduction method	-	4-NTP	CRISPR-/Cas12a-Mediated Liposome-Amplified detection	Duck meat	-	100 aM	-	-	+	[75]
Additives	6-BAP	AuNPs	Sodium citrate reduction method	-	-	6-BAP/AuNPs	Bean sprouts	-	0.33 μg·mL^{-1}	<5 min	-	+	[76]
Additives	Sodium sulfocyanate, melamine, dicyandiamide	AgNPs	Sodium citrate reduction method	-	-	AgNPs deposited chitosan-modified filter paper	Spiked milk powder	150	Sodium sulfocyanate: 10 mg·L^{-1} Melamine: 1 mg·L^{-1}, dicyandiamide: 100 mg·L^{-1}	<35 min	-	+	[77]
Dyes	MG, CV	Au@Ag core–shell Nps	Seed-mediated growth method	-	4-MBA	Au@4-MBA@Ag NRs decorated lab-on-capillary	Spiked shell	2.75×10^{6}	0.05 μM	-	-	+	[78]

Table 3 (continued)

Category of the pollutant	Pollutant	SERS substrate	Synthesis of the SERS substrate	Recognition element	Raman reporter molecule	Total SERS probe	Sample	EF	LOD	Detection time	Data analysis	On-site detection	Ref
Dyes and pesticide	CV, thiram	AgNPs	Sodium citrate reduction method	-	-	Paper-based Ag@SiO_2 core–shell NPs	-	-	10^{-9} M for thiram	-	-	+	[79]
Heavy metals	Zn^{2+}	AgNPs	Lee-Meisel method	Xylenol orange	-	AgNPs@ xylenol orange	Freshwater	-	200 nM	-	PLS analysis	+	[80]
Heavy metals	Cr(VI)	AgNPs	Sodium citrate reduction method	-	-	AgNPs	Spiked moat and spring water	-	0.72 ppb	-	-	+	[81]

4-NTP, 4-nitrothiophenol; *6-BAP*, 6-benzylaminopurine; *AgNPs*, silver nanoparticles; *AuNPs*, gold nanoparticles; *AuNRs*, gold nanorods; *AT*, ampicillin trihydrate; *Bap*, benzo[a]pyrene; *β-CD*, β-cyclodextrin; *CIP*, ciprofloxacin; *CPF*, chlorpyrifos; *Cr(VI)*, hexavalent chromium; *CV*, crystal violet; *EF*, enhancement factor; *GO*, graphene oxide; *LOD*, limit of detection; *MLR*, multiple linear regression; *MG*, malachite green; *NC*, nitrocellulose; *OHC*, oxytetracycline hydrochloride; *OTC*, oxytetracycline; *PAH*, polyaromatic hydrocarbons; *PCB*, polychlorinated biphenyl; *PLS*, partial least square; *SERS*, surface-enhanced Raman scattering; *SD*, sulfadiazine; *SDD*, sulfadimidine; *SMM*, sulfamonomethoxine; *TBZ*, thiabendazole; *TH*, tetracycline hydrochloride

hormones are used to change the maturation properties of the food, and there are also other types of additives used for different purposes.

Among additives, melamine is largely used in many foods, including pet food, milk, infant formula, to alter the protein content. It includes nitrogen at a 66% rate by mass, altering the measured protein content of the food [91, 92]. However, melamine can cause many health problems, including renal failure and death. According to the WHO report, in 2011, more than 50,000 children were hospitalized, and 6 children died due to the melamine found in infant formula in China [54]. Thus, the amount of melamine is restricted with a safety limit of 1 $\mu g \cdot L^{-1}$ for infant formula and 2.5 $\mu g \cdot L^{-1}$ for milk and food products [91–93].

For the detection of melamine, SERS is also used as a portable method with simple or no sample preparation methods. Wu et al. [94] determined the melamine and methyl parathion (MP) from the lake water and milk samples via SERS using a portable Raman spectrometer. AuNPs were used as SERS substrate and a wax-coated silicon wafer as a hydrophobic surface to enhance the aggregation of the AuNPs. AuNPs were mixed with melamine or MP and dropped on the wafer for the measurement. After drying, another layer of AuNPs was added to form a double-decker structure to enhance the formation of more hot spots. With that approach, they have detected melamine at least 10^{-9} M concentration. For the real lake water and milk samples, recovery rates of melamine were achieved in between 97.3–114.2% and 59.3–68.6% for lake water and milk samples, respectively.

Raveendran et al. [95] also used SERS to detect melamine and thiram, while they used microelectrode-templated silver nanodendrites as a detection platform. They used a handheld Raman spectrometer to demonstrate on-site detection from spiked apple juice samples. SERS substrate was formed on a microelectrode platform using electrochemical deposition with an alternating current signal. Grown silver nanodendrites inside the microelectrode provided detection of both melamine and thiram at 1 ppm in apple juice. When PCA was applied to observe the discrimination, completely separated groups were achieved between the control and thiram spiked groups for apple juice samples with 100% accuracy.

As a recent and different study, Ge et al. [96] used SERS for melamine and formaldehyde identification in melamine kitchenware. As a SERS probe, an aptamer derivatization-based membrane was developed. Firstly, composites of Ag^{+}-adsorbed SiO_2 spheres, reduced graphene oxide, and AgNPs were filtered through filter paper and then incubated with 3-methyl-2-benzothiazolinone hydrazone hydrochloride monohydrate (MBTH) as shown in Fig. 4A. MBTH was used for the derivatization of formaldehyde with a characteristic SERS peak.

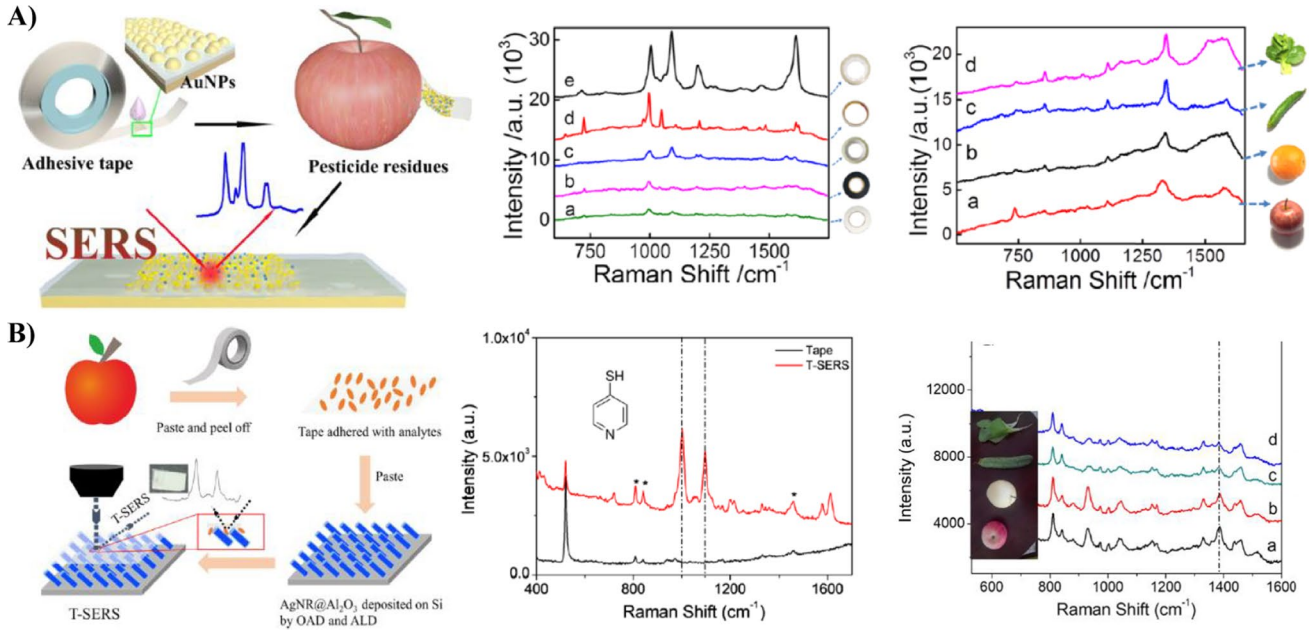

Fig. 3 SERS-based on-site detection of pesticides. **A** Detection of pesticides from different food with the paste and peel method of the SERS-tape, which is based on the AuNPs dropped tape with the direct measurement on the tape. Reproduced with permission from Ref. [8]. Copyright 2016 American Chemical Society. **B** On-site detection of tetramethylthiuram disulfide (TMTD) and thiabendazole (TBZ) from the apple peel using Al_2O_3-coated AgNRs array and tape-based extraction. Reproduced with permission from Ref. [87]. Copyright 2018 American Chemical Society

Reduced GO was used to increase the loading efficiency of AgNPs, adsorption of MBTH and formaldehyde, reduce oxidation of AgNPs with enhanced stability, and induce charge transfer enhancement mechanism. Then, formed membranes were modified with melamine aptamer prior to the measurement. Melamine and formaldehyde migrations from melamine kitchenware, dish, spoon, and bowl were tracked, and melamine and formaldehyde were found under simulated acid conditions. Detection accuracy was compared using HPLC, where results showed a difference less than 5.2%. LOD of melamine was found as 0.15 mg·L^{-1}, and LOD of formaldehyde was 1.21 mg·L^{-1}, while recovery rates ranged from 91.2 to 110.0% and 94.0 to 106.0%, respectively. The proposed report showed a real application of SERS on the detection of migrated melamine from frequently used kitchenware.

Additives other than melamine are also used for different purposes. For instance, there are illegal adulterants used in botanical dietary supplements due to being similar to the supplements. Diphenhydramine hydrochloride (DIP), benproperine phosphate (BEN), and chlorphenamine maleate (CHL) are among the illegal adulterants where Fang et al. [97] used thin-layer chromatography (TLC) combined SERS for their detection. For the detection, samples were spotted on the TLC plate and eluted. When eluent is evaporated on the TLC plate, SERS signals were obtained with the addition of AgNPs colloids. LOD of the developed method was 0.01 μg·mL^{-1} for both DIP and BEN and 0.005 μg·mL^{-1} for CHL in solutions. Ten botanical dietary supplements, including 3 tablets, 4 granules, and 3 capsules, were used as real samples. It was observed that one of the samples has a similar behavior on the TLC and SERS spectra with BEN reference sample. When they checked the adulterant levels of that sample with UPLC-MS, they have found that mentioned sample is doped with BEN and the designed TLC-coupled SERS method can detect adulterants from the real sample without any spiking.

Illegal adulteration is not obtained only by the addition of chemical adulterants but also by gene editing. As an adulteration process, Liu et al. [75] detected not a direct pollutant but an adulterated duck gene using SERS (Fig. 4C). They have proposed a CRISPR/Cas12a-mediated liposome-amplified strategy for SERS and naked-eye detection of target nucleic acid. For the production of the proposed system, biotin and NH_2 modified 90mer timin ssDNA was grafted on bovine serum albumin (BSA)-coated well plate. Then, clustered regularly interspaced short palindromic repeats (CRISPR) and CRISPR-associated (Cas) 12a reaction system was added on the plate. When there was no target DNA, the trans-cleavage activity of Cas12a was inhibited, and ssDNA remained in the plate. However, when target DNA is added onto the plate, with the recognition of

target DNA by guide CRISPR RNA, ssDNA is cleaved from the plate, which provided a decrease in the concentration of ssDNA. When the supernatant with cleaved ssDNA is removed from the wells of the plate, only the unbroken and remaining ssDNA could be captured by Raman reporter molecule-loaded liposomes via biotin-streptavidin chemistry. Thus, when liposomes were ruptured with a surfactant and AuNPs were added to the wells, obtained SERS signal from the reporter provides the presence of target DNA. Furthermore, cysteine was used for naked-eye detection, which provided AuNPs aggregation with a color change from red to blue due to the SPR shift of aggregated AuNPs. Even the proposed system has a complex structure and many steps for the detection, it provided LOD as 100 aM for the SERS measurement and 10 pM for the naked-eye detection. They have also detected the DNA from the lamb roll, pork, beef, mutton, and steak samples with spiking adulterated duck meat in samples. They have calculated the recovery rates between 90.26 and 103.20%, which shows the ability of the proposed method to detect DNA to track the addition of adulterants by gene editing from the real samples with high selectivity.

As another adulterant, 6-benzylaminopurine (6-Bap) is used as synthetic cytokinin for plant growth with the stimulation of plant cell division. Zhang et al. [76] used SERS with the help of AuNPs colloid to detect 6-Bap. Mung bean seeds were used as the sample, and 4 different extraction methods were examined: grinding, solvent, ultrasonic, and fast solid-phase extraction methods. Among all extraction methods, grinding extraction provided simpler, faster extraction without any special equipment with more sensitive results. The total measurement took 5 min where extracts were directly mixed with AuNPs, and measurements were obtained immediately from the mixture using a portable Raman spectrometer. The lowest detectable concentration of 6-Bap was found as 0.33 $\mu g \cdot mL^{-1}$. The accuracy of the results was investigated by comparing results with the HPLC. Even they did not provide detailed information about the comparison with a validated method, they showed that consistent data was observed between the two methods.

Yang et al. [9] used SERS for the identification of phthalate plasticizers. Instead of using nanoparticles directly for the detection, they designed an electrochemically reduced MoS_2-modified electrode decorated with molecularly imprinted polymer-based core–shell AuNP polydopamine nanoparticles. The proposed system provided electrokinetic pre-separation, trapping of charged molecules, and reduction in nonspecific binding, as seen in Fig. 4B. The use of an electric field provided separation of similarly charged molecules and concentration of the oppositely charged molecules. They have used this system for the detection of two plasticizers, dimethyl phthalate (DMP) and di(2-ethylhexyl) phthalate (DEHP), where they were detected with a detection limit as low as 2.7×10^{-12} M and 2.3×10^{-11} M, respectively from plastic bottled water.

Illegal dyes were also used as additives to change the color of the foods. As a recent example, Guo et al. [98] detected malachite green (MG) dye with flexible Nafion membrane stabilized Ag nanopillar arrays. They have used colloidal lithography to self-assemble polystyrene (PS) monolayer on a Nafion membrane. Then, nanopillar structures were obtained with the ion plasma etching of membranes. To have a SERS substrate in the system, they have coated a layer of Ag on the surface of the membrane with ionic exchange and in situ chemical reduction. The formed array structure provided 2.8×10^6 and 3.07×10^6 EF for two different Raman bands of the 4-ATP using a portable Raman spectrometer. Even they did not use this flexible structure to detect a real sample; they proposed that their system can be applied to the outdoor on-site detection of pollutants.

Lin et al. [78] also detected MG and CV dye via SERS using a lab-on-capillary platform. To fabricate the capillary-based platform, pentatwinned Au nanobipyramids were synthesized and used as seeds for the formation of AuNRs. Then, AuNRs were modified with 4-MBA and coated with Ag layer as Au core Ag shell nanorods. The synthesized SERS probe was coated to the inner wall of a capillary tube with a homogenous and dense distribution. They have also designed a homemade system for the on-site detection from real samples. The shell was used as a real sample, and it was spiked with CV and MG, and then the designed capillary platform was used to extract the dye from the surface of the shell. The detection limit was achieved as 0.05 μM for both of the dyes with the developed homemade system.

As a more recent example, Kong et al. [99] developed a graphene oxide silver-coated Au nanobones mixture which is decorated on a cellulose membrane for the detection of various colorants, including rhodamine B (RB), auramine O (AO), malachite green (MG), carmine (CM), sunset yellow (SY), brilliant blue (BB). Enhancement factor with the R6G was calculated as 1.76×10^6 where detectable least concentration for R6G was found as 1.12×10^{-9} M. LOD and LOQ values for 6 different colorants were found in a range between 0.010–1.1 $\mu g \cdot cm^{-2}$ and 0.011–1.56 $\mu g \cdot cm^{-2}$, respectively. When SVM was used as a multivariate analysis, they have observed that six different colorants can be identified and classified with 88.9–100% accuracy. They used energy drink and bayberry wine for the detection of dyes. Beverages were loaded into the decorated cellulose membranes, and SERS measurements showed that BB dye could be detected inside the energy beverage and CM dye inside the bayberry wine.

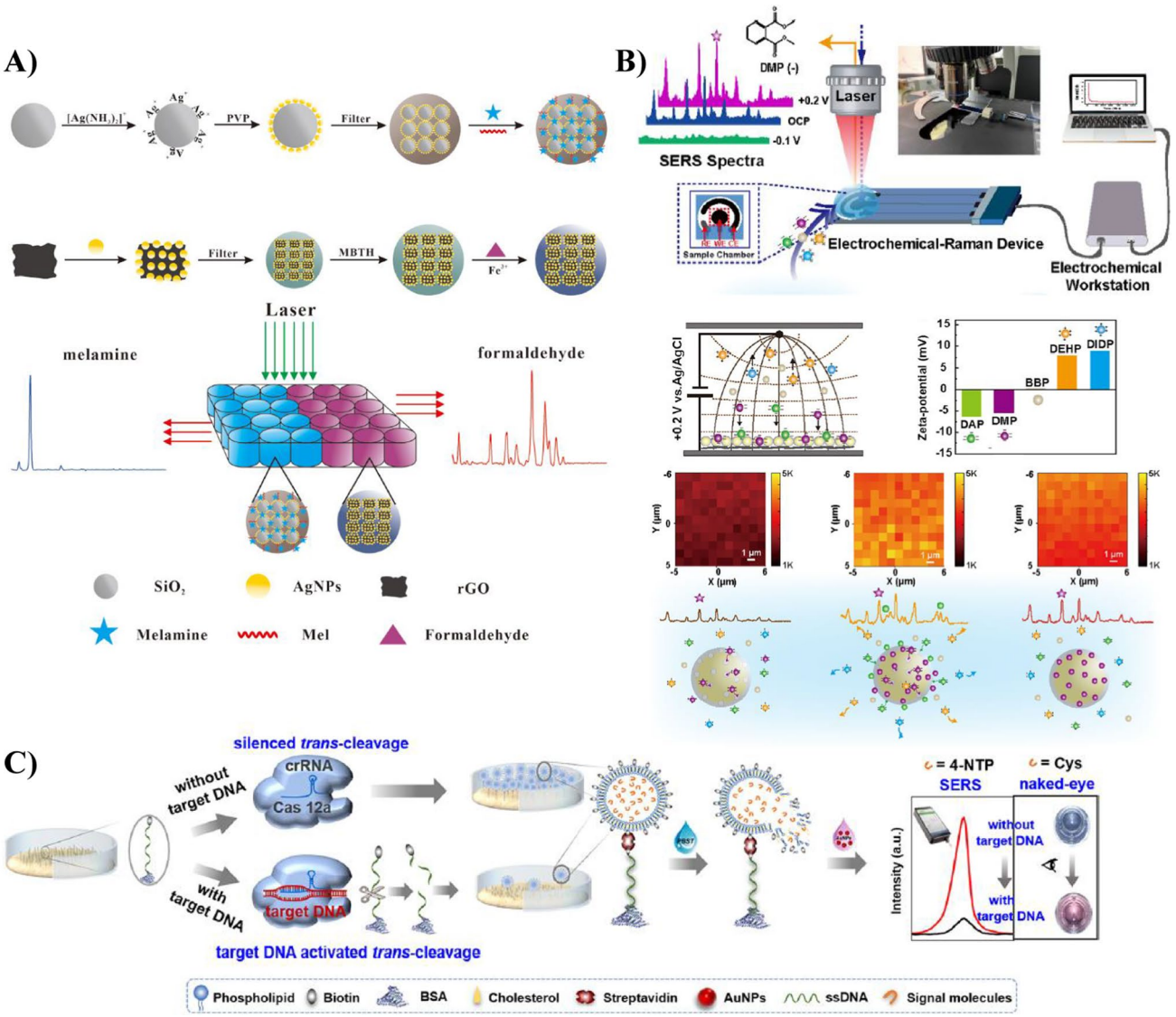

Fig. 4 SERS-based on-site detection of additives. **A** Detection of melamine and formaldehyde in melamine kitchenware using melamine aptamer modified membrane consisting of Ag^+ adsorbed SiO_2 spheres, reduced graphene oxide, and AgNPs. Reproduced from Ref. [96]. Copyright 2021 Elsevier. **B** Detection of phthalate plasticizers with molecularly imprinted polymer-based core–shell AuNP polydopamine nanoparticles immobilized on an electrochemically reduced MoS_2-modified electrode. Reproduced from Ref. [9]. Copyright 2021 American Chemical Society. **C** Development of a CRISPR/Cas12a-mediated liposome-amplified strategy for the detection of adulterated duck gene by SERS. Reproduced from Ref. [75]. Copyright 2021 American Chemical Society

5 Detection of microplastics as physical pollutants

Production and consumption of plastics have been increasing exponentially worldwide, which are used in many different industries, including textile, cosmetics, washing industry, and personal care products. Three hundred million tons of plastics on a global scale were produced. Among them, approximately ten thousand tons ended up in the water and oceans, where their accumulation is predicted as hundreds of millions of tons by 2025 [100–102]. They are discharged to the environment by sewage treatment plants, fisheries, and water operation industries [103], and they have been found in the marine water, freshwater, agroecosystems, the atmosphere, food, drinking water, and biota [104–106]. Their non-degradable nature threatens the environment, ecosystem, and human health, and the toxicity comes from not only directly plastics but also from the molecules that are adsorbed by the microplastics such as antibiotics, heavy metals, and organic pollutants, which lead to long-range migration and more complex effects [107]. They can enter the human body via the ingestion of contaminated food [108,

Table 4 SERS-based detection of microplastics

Category of the pollutant	Pollutant	SERS substrate	Synthesis of the SERS substrate	Recognition element	Raman reporter molecule	Total SERS probe	Sample	EF	LOD	Detection time	Data analysis	On-site detection	Ref
Nanoparticles	AgNPs	Au slides	Purchased	Ferbam	-	Au slides@ferbam	Throat spray (A), antibacterial hydrogel (B), nasal spray (C), antifungal spray (D)	-	A: 21.5 $mg{\cdot}L^{-1}$, B: 20.0 $mg{\cdot}kg^{-1}$, C: 10.0 $mg{\cdot}L^{-1}$, D: 6.5 $mg{\cdot}L^{-1}$	-	-	-	[124]
Nanoparticles	AgNPs	AgNPs	Purchased	Ferbam	-	AgNPs@ferbam	Spiked environmental water, wheat plants	-	2 $\mu g{\cdot}g^{-1}$ in wheat plants	~25 min	-	-	[125]
Nanoparticles	AgNPs	AgNPs	Purchased	-	4-MBA	AgNPs@4-MBA	Wheat leaf	-	2 $\mu g{\cdot}g^{-1}$	-	-	-	[127]
Microplastics	PP, PE, PS	AgNPs	Sodium citrate reduction method	-	-	AgNPs	Pure water and seawater	4×10^4	40 $\mu g{\cdot}mL^{-1}$ for 100 nm PS	-	-	+	[119]
Microplastics	PS, PMMA	Au Klarite	Purchased	-	-	Au Klarite	Atmospheric aerosol particles extracted from the air in Shanghai	172 ± 22	-	-	-	-	[128]
Microplastics	PS, PET, PE, PVC, PP	AuNPs	Sodium citrate reduction method	-	4-MPY	AuNPs decorated styrene-butadiene latex sponge	Snow water, seawater, river water, and rainwater	1.39×10^9	0.001 $mg{\cdot}mL^{-1}$	-	-	+	[120]
Nanoplastics	PS	AgNPs	Hydroxylamine reduction method	-	-	AgNPs	Spiked water samples from Kunyu river	-	-	-	-	-	[129]
Microplastics	PS	Gold nanostars (AuNSs)@Ag	Sodium citrate reduction method	-	-	Anisotropic nanostar dimer-embedded nanopore	The tap, river, and seawater samples	-	0.05%	A few min	Finite element method	-	[130]

Table 4 (continued)

Category of the pollutant	Pollutant	SERS substrate	Synthesis of the SERS substrate	Recognition element	Raman reporter molecule	Total SERS probe	Sample	EF	LOD	Detection time	Data analysis	On-site detection	Ref
Micro/nanoplastics	PS, PET	AuNPs	Sodium citrate and hydroxylamine reduction method	-	-	AuNPs	Fish and shellfish samples	446	10 μg·mL^{-1}		-	-	[131]
Nanoplastics	PS	AuNRs, AgNWs	Polyol method	-	-	Cellulose hydrogel assisted AuNRs and AgNWs	-	1.8×10^{7}	0.1 mg·mL^{-1}	-	-	-	[132]

4-MBA, 4-mercaptobenzoic acid; *4-MPY*, 4-mercaptopyridine; *AgNPs*, silver nanoparticles; *AgNWs*, silver nanowires; *AuNPs*, gold nanoparticles; *AuNRs*, gold nanorods; *AuNSs*, gold nanostars; *EF*, enhancement factor; *ferbam*, ferric dimethyl-dithiocarbamat; *LOD*, limit of detection; *PE*, polyethylene; *PET*, poly(ethylene terephthalate); *PMMA*, poly(methyl methacrylate); *PP*, polypropylene; *PS*, polystyrene; *PVC*, poly(vinyl chloride); *SERS*, surface-enhanced Raman scattering

109], inhalation [110], and even skin contact when the size is down to nanoscale [111]. Exposure to the microplastics can affect the neural [112], digestive, excretory [113–115], and respiratory system [116, 117].

There are studies in the literature to detect microplastics, but alternative method development strategies are limited due to being a more recent concern. Most SERS-based detection studies use laboratory-type Raman spectrometers, which are not suitable for on-site detection. A few examples of the on-site detection systems are given in Table 4 with the laboratory-type examples**.**

As an example of a portable on-site detection system, Iri et al. [118] designed a portable Raman spectrometer prototype for the identification of microplastics. They used a quartz cuvette as the holder of the water samples, shown in Fig. 5A. Characteristic Raman peaks of the microparticles were investigated without any enhancement, and when they checked the detection ability of the designed spectrometer, their system provided linear relation in between 0.015 and 0.035% w/v. On the other hand, using only the Raman signal did not provide significant information about the microplastics in water.

Lv et al. [119] used silver colloids to enhance the obtained Raman signal from nanoforms of PS, polyethylene (PE), polypropylene (PP) in water. Silver colloids were prepared by Lee and Meisel's chemical reduction method, and seawater was used as the sample where plastics were dispersed. They have compared the obtained Raman signal in the absence of silver colloids with the SERS signal in the presence of silver colloids. Compared with Iri et al., more than two peaks of microplastics were enhanced with the presence of AgNPs. EF of the AgNPs was calculated as 5×10^{2} for the 100 nm PS spheres while it was 4×10^{4} for 500 nm PS spheres. When they compared the measurement in the pure water and seawater, they observed similar trends in the obtained spectra, and the signal from the PS sphere was not disturbed by the matrix. With the use of a portable Raman spectrometer, 40 μg·mL^{-1} of 100 nm plastics were determined, which is claimed as a good selectivity to detect released plastics in the aquatic environments.

Yin et al. [120] detected trace microplastics in non-pretreated water samples using a sponge-supported Au nanoparticle layer. The sponge-based substrate provided capturing and concentrating of the microplastics from the sample, and it was fabricated by the layer-by-layer assembly. Developed SERS substrate provided EF as 1.39×10^{9} when 4-mercaptopyridine (4-MPY) was used as a reporter molecule, and LOD was found as 0.001 mg·mL^{-1} for microplastics. For the real sample applications, snow water, seawater, river water, and rainwater were used, and a good linear correlation in the range between 0.05–100 mg·mL^{-1} concentration was achieved.

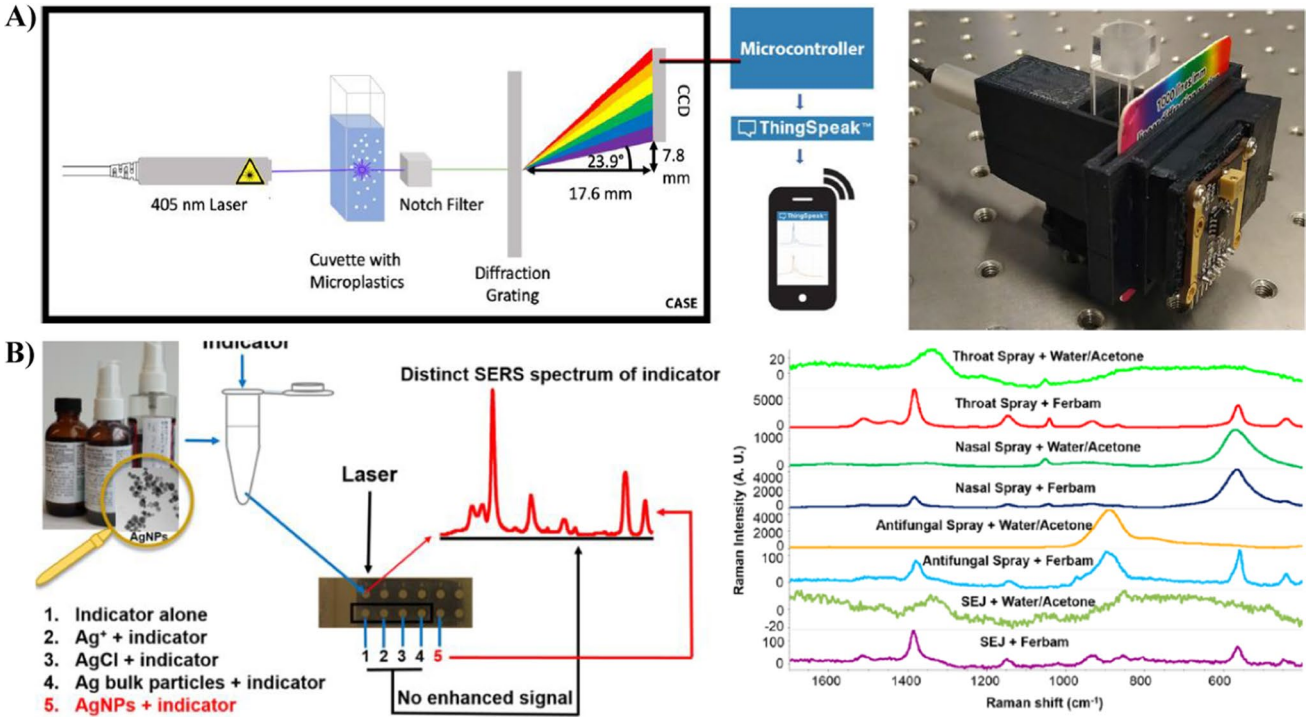

Fig. 5 SERS-based detection of micro/nanoplastics. **A** Development of a portable Raman system for the detection of microparticles. Reproduced with permission from Ref. [118]. Copyright 2021 Springer Nature. **B** Detection of AgNPs inside the antimicrobial products; throat spray, nasal spray, disinfecting spray, and hydrogel, with an indicator (ferbam) of nanoparticles which provides Raman signal and strong binding to AgNPs. Reproduced with permission from Ref. [124]. Copyright 2015 American Chemical Society

Not only microplastics but also synthesized nanoparticles were also started to be a concern as environmental pollution. Large-scale use of nanoparticles in different products and sectors, including cosmetics, textiles, electronics, household products, and purification, sanitation technologies, brings up exposure and toxicity issues [121]. For example, exposure to the AgNPs through ingestion, inhalation, or dermal routes could cause inflammation in the respiratory and cardiovascular systems, leading to chronic bronchitis, respiratory tract irritation, and infection [122]. Thus, exposure limits were defined for the particles by the National Institute for Occupational Safety and Health (NIOSH) as 10 $mg{\cdot}m^{-3}$ for silver compounds. Moreover, EPA defined a secondary standard for the inhalable particles, which is described by particulate matter (PM) with a size definition, which is 12.0 $\mu g{\cdot}m^{-3}$ and 15.0 $\mu g{\cdot}m^{-3}$ for $PM_{2.5}$ and PM_{10}, respectively [123]. Thus, not only the use of nanoparticles for the detection of agricultural pollutants but also their own detection from the environment is also crucial.

Guo et al. [124] detected the AgNPs in antimicrobial products using SERS. Ferric dimethyl-dithiocarbamate (ferbam) was used as an indicator of AgNPs, and as pollutant, citrate and PVP-coated AgNPs were selected. Due to their strong interaction with ferbam, effective detection of AgNPs has been achieved in size range between 20 to 200 nm. 4 different antimicrobial products, throat spray, which is labeled with the presence of colloidal silver, a nasal spray, which contains colloidal silver, a disinfecting spray, which is based on the 99.99% pure colloidal silver, and an antibacterial hydrogel, which is labeled as nanosilver hydrogel, was examined for the presence of AgNPs as shown in Fig. 5B. SERS results were validated with ICP-MS results, and it was found that closer results were obtained to the ICP-MS results with the developed SERS-based detection system, while size variation of AgNPs inside the products affected the obtained SERS spectra.

The same group developed another detections strategy using a filter-based method to improve the detection sensitivity [125]. For the measurement, AgNPs were first filtered through a syringe filter firstly. Then, the analyte was mixed with $CaCl_2$ and $AlCl_3$ for the AgNPs aggregation. Similar to the previous method, ferbam was used as a reporter molecule via filtering through the membrane. Then, the membrane was removed, dried, and the signal was measured. When they have compared the filtration-based detection method with the centrifugation-based detection method, 20-fold lower LOD was achieved as

5 $\mu g \cdot L^{-1}$. Trace levels of AgNPs were also detected from the pond water at 10 $\mu g \cdot L^{-1}$ concentration.

As a more recent study, Quaratova et al. [126] detected AgNPs in seawater with a portable Raman system. They detected various sized, PVP-coated AgNPs, and 4-ABT functionalized Au nanostars (AuNSs) was used as SERS substrate. 4-ABT was used as the reporter and chemoreceptor to trap the AgNPs. AgNPs and AuNSs were mixed, and measurements were obtained without drying. The detection limit was achieved at 1.51 $\mu g \cdot L^{-1}$ in seawater. They have concluded that a portable device with a sample preparation module could reduce the challenges of detecting real samples and increase specificity when SERS is used as the on-site detection method.

6 Conclusion

Environmental pollutants become an essential issue day after day with increasing population, production, and consumption. Detection of pollutants from the field is also crucial to directly understand the level of pollutants outdoor, which is essential to determine the exposure of the environment, wildlife, and humans leading to different diseases and even death. It is also important for the sale of the products, which should encounter the regulations of the presence of pollutants. Thus, fast, portable detection systems are required. However, common methods used to detect agricultural pollutants are mainly found in laboratories without any ability to use them on-site outdoor detection. As an alternative, SERS can be used as a fast and portable method when portable detection systems are developed and used with a portable spectrometer. It does not require long and complex sample preparation steps and can provide detection at a low detection time. In this review, on-site detection applications of SERS reviewed for biological, chemical, and physical agricultural pollutants. Mechanisms of SERS, along with the type of SERS substrates, were also underlined. There are reports on on-site detection of agricultural pollutants, including the development of portable systems, detection with a portable spectrometer, or detection from real samples; however, examples that combine real sample measurements with portable system and spectrometers are limited for most of the pollutants. On the other hand, reported studies mostly focused on observing the SERS spectra in the field. However, not only getting spectra but also getting the information from the spectra on-site is also crucial. If portable systems can be integrated with such systems as artificial intelligence, obtained results could directly show the pollutant and also the amount without any further interpretation. Moreover, most of the studies are based on the detection from solutions or some part of the foods (peels); however, it should be noted that most of the pollutants can also be found inside the foods, as seen in the systemic pesticide examples. Thus, even there are reports based on the on-site detection of agricultural pollutants, further studies are needed to examine the real examples with simple, fast, sensitive, and selective methods that combine portable detection prototypes with a portable spectrometer.

Declarations

Conflict of interest The authors declare no competing interests.

References

1. World Health Organization, Water, sanitation and hygiene, World Health Organization. (2015). https://www.who.int/health-topics/water-sanitation-and-hygiene-wash. Accessed 29 Nov 2021
2. World Health Organization, Food safety food safety, World Health Organization. (2013). https://www.who.int/health-topics/food-safety. Accessed 17 Dec 2021
3. J.W.-F. Law, N.-S. Ab Mutalib, K.-G. Chan, L.-H. Lee, Rapid methods for the detection of foodborne bacterial pathogens: principles, applications, advantages and limitations. Front. Microbiol. **5**, 1–19 (2015). https://doi.org/10.3389/fmicb.2014.00770
4. S. Baruah, J. Dutta, Nanotechnology applications in pollution sensing and degradation in agriculture: a review. Environ. Chem. Lett. **7**(3), 191–204 (2009). https://doi.org/10.1007/s10311-009-0228-8
5. B. Sharma, R.R. Frontiera, A.I. Henry, E. Ringe, R.P. Van Duyne, SERS: materials, applications, and the future. Mater. Today **15**(1–2), 16–25 (2012). https://doi.org/10.1016/S1369-7021(12)70017-2
6. B. Krafft, A. Tycova, R.D. Urban, C. Dusny, D. Belder, Microfluidic device for concentration and SERS-based detection of bacteria in drinking water. Electrophoresis **42**(1–2), 86–94 (2021). https://doi.org/10.1002/elps.202000048
7. M. Xiao et al., Ultrasensitive detection of avian influenza A (H7N9) virus using surface-enhanced Raman scattering-based lateral flow immunoassay strips. Anal. Chim. Acta **1053**, 139–147 (2019). https://doi.org/10.1016/j.aca.2018.11.056
8. J. Chen et al., Flexible and adhesive surface enhance Raman scattering active tape for rapid detection of pesticide residues in fruits and vegetables. Anal. Chem. **88**(4), 2149–2155 (2016). https://doi.org/10.1021/acs.analchem.5b03735
9. Y. Yang et al., Electrokinetic preseparation and molecularly imprinted trapping for highly selective SERS detection of charged phthalate plasticizers. Anal. Chem. **93**(2), 946–955 (2021). https://doi.org/10.1021/acs.analchem.0c03652
10. Z. Lin, L. He, Recent advance in SERS techniques for food safety and quality analysis: a brief review. Curr. Opin. Food Sci. **28**, 82–87 (2019). https://doi.org/10.1016/j.cofs.2019.10.001
11. D.-W. Li, W.-L. Zhai, Y.-T. Li, Y.-T. Long, Recent progress in surface enhanced Raman spectroscopy for the detection of environmental pollutants. Microchim. Acta **181**(1–2), 23–43 (2014). https://doi.org/10.1007/s00604-013-1115-3
12. M. Petersen, Z. Yu, X. Lu, Application of Raman spectroscopic methods in food safety: a review. Biosensors **11**(6), 1–22 (2021). https://doi.org/10.3390/bios11060187
13. Y. Guo et al., Rapid and ultrasensitive detection of food contaminants using surface-enhanced Raman spectroscopy-based

methods. Crit. Rev. Food Sci. Nutr. **61**(21), 3555–3568 (2021). https://doi.org/10.1080/10408398.2020.1803197
14. R. Gillibert, J.Q. Huang, Y. Zhang, W.L. Fu, M. Lamy de la Chapelle, Food quality control by surface enhanced Raman scattering. TrAC Trends Anal. Chem. **105**, 185–190 (2018). https://doi.org/10.1016/j.trac.2018.05.009
15. A.P. Craig, A.S. Franca, J. Irudayaraj, Surface-enhanced Raman spectroscopy applied to food safety. Annu. Rev. Food Sci. Technol. **4**(1), 369–380 (2013). https://doi.org/10.1146/annurev-food-022811-101227
16. X. Zhao, M. Li, Z. Xu, Detection of foodborne pathogens by surface enhanced Raman spectroscopy. Front. Microbiol. **9**, 1–13 (2018). https://doi.org/10.3389/fmicb.2018.01236
17. C.V. Raman, K.S. Krishnan, A new type of secondary radiation. Nature **121**(3048), 501–502 (1928). https://doi.org/10.1038/121501c0
18. L. Zhao, L. Jensen, G.C. Schatz, Pyridine-Ag20 cluster: a model system for studying surface-enhanced Raman scattering. J. Am. Chem. Soc. **128**(9), 2911–2919 (2006). https://doi.org/10.1021/ja0556326
19. M. Fleischmann, P.J. Hendra, A.J. McQuillan, Raman spectra of pyridine adsorbed at a silver electrode. Chem. Phys. Lett. **26**(2), 163–166 (1974). https://doi.org/10.1016/0009-2614(74)85388-1
20. D.L. Jeanmaire, R.P. Van Duyne, Surface raman spectroelectrochemistry. Part I. Heterocyclic, aromatic, and aliphatic amines adsorbed on the anodized silver electrode. J. Electroanal. Chem. **84**(1), 1–20 (1977). https://doi.org/10.1016/S0022-0728(77)80224-6
21. M.G. Albrecht, J.A. Creighton, Anomalously intense Raman spectra of pyridine at a silver electrode. J. Am. Chem. Soc. **99**(15), 5215–5217 (1977). https://doi.org/10.1021/ja00457a071
22. G.C. Schatz, R.P. Van Duyne, Electromagnetic mechanism of surface-enhanced spectroscopy. Handb. Vib. Spectrosc. (2006). https://doi.org/10.1002/0470027320.s0601
23. L. Xia et al., Visualized method of chemical enhancement mechanism on SERS and TERS. J. Raman Spectrosc. **45**(7), 533–540 (2014). https://doi.org/10.1002/jrs.4504
24. H. Tang, C. Zhu, G. Meng, N. Wu, Review—Surface-enhanced Raman scattering sensors for food safety and environmental monitoring. J. Electrochem. Soc. **165**(8), B3098–B3118 (2018). https://doi.org/10.1149/2.0161808jes
25. H. C. Gugnani. Some emerging food and water borne pathogens. J. Commun. Dis. **31**(2), 65–72 (1999), Accessed: Nov. 24, 2021. [Online]. Available: https://europepmc.org/article/med/10810592
26. S. Sharma, P. Sachdeva, J.S. Virdi, Emerging water-borne pathogens. Appl. Microbiol. Biotechnol. **61**(5–6), 424–428 (2003). https://doi.org/10.1007/s00253-003-1302-y
27. M. Rippa et al., SERS biosensor based on engineered 2D-Aperiodic nanostructure for in-situ detection of viable Brucella bacterium in complex matrix. Nanomaterials **11**(4), 886 (2021). https://doi.org/10.3390/nano11040886
28. S.H. Hilton, C. Hall, H.T. Nguyen, M.L. Everitt, P. DeShong, I.M. White, Phenotypically distinguishing ESBL-producing pathogens using paper-based surface enhanced Raman sensors. Anal. Chim. Acta **1127**, 207–216 (2020). https://doi.org/10.1016/j.aca.2020.06.068
29. Y. Liu, H. Yu, Y. Cheng, Y. Guo, W. Yao, Y. Xie, Nondestructive monitoring of *Staphylococcus aureus* biofilm by surface-enhanced Raman scattering spectroscopy. Food Anal. Methods **13**(9), 1710–1716 (2020). https://doi.org/10.1007/s12161-020-01792-6
30. C. Pan, B. Zhu, C. Yu, A Dual Immunological Raman-Enabled Crosschecking Test (DIRECT) for detection of bacteria in low moisture food. Biosensors **10**(12), 200 (2020). https://doi.org/10.3390/bios10120200
31. Y. Zhou et al., Terminal deoxynucleotidyl transferase (TdT)-catalyzed homo-nucleotides-constituted ssDNA: inducing tunable-size nanogap for core-shell plasmonic metal nanostructure and acting as Raman reporters for detection of *Escherichia coli* O157:H7. Biosens. Bioelectron. **141**, 111419 (2019). https://doi.org/10.1016/j.bios.2019.111419
32. R. Wang et al., Highly sensitive detection of high-risk bacterial pathogens using SERS-based lateral flow assay strips. Sensors Actuators B Chem. **270**, 72–79 (2018). https://doi.org/10.1016/j.snb.2018.04.162
33. H. Li, C. Li, F.L. Martin, D. Zhang, Diagnose Pathogens in drinking water via magnetic Surface-Enhanced Raman Scattering (SERS) Assay. Mater. Today Proc. **4**(1), 25–31 (2017). https://doi.org/10.1016/j.matpr.2017.01.189
34. A.H. Arslan, F.U. Ciloglu, U. Yilmaz, E. Simsek, O. Aydin, Discrimination of waterborne pathogens, *Cryptosporidium parvum* oocysts and bacteria using surface-enhanced Raman spectroscopy coupled with principal component analysis and hierarchical clustering, *Spectrochim*. Acta Part A Mol. Biomol. Spectrosc. **267**, 120475 (2022). https://doi.org/10.1016/j.saa.2021.120475
35. G. Palermo et al., Plasmonic metasurfaces based on pyramidal nanoholes for high-efficiency SERS biosensing. ACS Appl. Mater. Interfaces **13**(36), 43715–43725 (2021). https://doi.org/10.1021/acsami.1c12525
36. D. Zhang et al., Ultra-fast and onsite interrogation of Severe Acute Respiratory Syndrome Coronavirus 2 (SARS-CoV-2) in waters via surface enhanced Raman scattering (SERS). Water Res. **200**, 117243 (2021). https://doi.org/10.1016/j.watres.2021.117243
37. S. Yadav, S. Senapati, D. Desai, S. Gahlaut, S. Kulkarni, J.P. Singh, Portable and sensitive Ag nanorods based SERS platform for rapid HIV-1 detection and tropism determination. Colloids Surfaces B Biointerfaces **198**, 111477 (2021). https://doi.org/10.1016/j.colsurfb.2020.111477
38. Y. Sun et al., A promising magnetic SERS immunosensor for sensitive detection of avian influenza virus. Biosens. Bioelectron. **89**, 906–912 (2017). https://doi.org/10.1016/j.bios.2016.09.100
39. M. Zhang et al., Ultrasensitive detection of SARS-CoV-2 spike protein in untreated saliva using SERS-based biosensor. Biosens. Bioelectron. **190**, 113421 (2021). https://doi.org/10.1016/j.bios.2021.113421
40. Q. Yu, Y. Wu, T. Kang, J. Choo, Development of surface-enhanced Raman scattering-based immunoassay platforms using hollow Au nanostars for reliable SARS-CoV-2 diagnosis. Bull Korean Chem Soc **42**(12), 1699–1705 (2021). https://doi.org/10.1002/bkcs.12418
41. K. Daoudi et al., Ultra-sensitive and fast optical detection of the spike protein of the SARS-CoV-2 using AgNPs/SiNWs nanohybrid based sensors. Surf. Interfaces **27**, 101454 (2021). https://doi.org/10.1016/j.surfin.2021.101454
42. H. Liu et al., Development of a SERS-based lateral flow immunoassay for rapid and ultra-sensitive detection of anti-SARS-CoV-2 IgM/IgG in clinical samples. Sensors Actuators B Chem. **329**, 129196 (2021). https://doi.org/10.1016/j.snb.2020.129196
43. O.J. Achadu et al., Sulfur-doped carbon dots@polydopamine-functionalized magnetic silver nanocubes for dual-modality detection of norovirus. Biosens. Bioelectron. **193**, 113540 (2021). https://doi.org/10.1016/j.bios.2021.113540
44. K. Rule Wigginton, P.J. Vikesland, Gold-coated polycarbonate membrane filter for pathogen concentration and SERS-based detection. Analyst **135**(6), 1320–1326 (2010). https://doi.org/10.1039/b919270k
45. Y. Wang et al., Duplex microfluidic SERS detection of pathogen antigens with nanoyeast single-chain variable fragments. Anal.

Chem. **86**(19), 9930–9938 (2014). https://doi.org/10.1021/ac5027012
46. K. Rule, P.J. Vikesland, Surface-enhanced resonance raman spectroscopy for the rapid detection of cryptosporidium parvum and giardia lamblia. Environ. Sci. Technol. **43**(4), 1147–1152 (2009). https://doi.org/10.1021/es801531t
47. K. Rebrošová et al., Rapid identification of staphylococci by Raman spectroscopy. Sci. Rep. **7**(1), 14846 (2017). https://doi.org/10.1038/s41598-017-13940-w
48. S. Jaafreh, O. Valler, J. Kreyenschmidt, K. Günther, P. Kaul, In vitro discrimination and classification of Microbial Flora of Poultry using two dispersive Raman spectrometers (microscope and Portable Fiber-Optic systems) in tandem with chemometric analysis. Talanta **202**, 411–425 (2019). https://doi.org/10.1016/j.talanta.2019.04.082
49. J. Hong et al., Rapid detection of pathogens using direct and surface enhanced Raman spectroscopy. Sens Agric Food Qual Saf XI **10**, (2019). https://doi.org/10.1117/12.2520624
50. C. Wang, F. Madiyar, C. Yu, J. Li, Detection of extremely low concentration waterborne pathogen using a multiplexing self-referencing SERS microfluidic biosensor. J. Biol. Eng. **11**(1), 1–11 (2017). https://doi.org/10.1186/s13036-017-0051-x
51. N. E. Dina, D. Marconi, A. Colniță, A. M. R. Gherman, Microfluidic portable device for pathogens 'rapid SERS detection, in Proceedings of The 1st International Electronic Conference on Biosensors 7089, (2020). https://doi.org/10.3390/IECB2020-07089
52. M. L. Bari, D. O. Ukuku, (Eds.). Foodborne Pathogens and Food Safety (1st ed.). CRC Press. (2015). https://doi.org/10.1201/b19851
53. C. Fan, Z. Hu, L.K. Riley, G.A. Purdy, A. Mustapha, M. Lin, Detecting Food- and waterborne viruses by surface-enhanced Raman spectroscopy. J. Food Sci. **75**(5), M302–M307 (2010). https://doi.org/10.1111/J.1750-3841.2010.01619.X
54. World Health Organisation, Melamine-contaminated powdered infant formula in China - update emergencies preparedness, response, World Health Organization, (2008). https://www.who.int/emergencies/disease-outbreak-news/item/2008_09_29a-en (accessed Dec. 17, 2021)
55. World Health Organization, Pesticide residues in food, World Health Organization. (2018). https://www.who.int/news-room/fact-sheets/detail/pesticide-residues-in-food. Accessed 26 Nov 2021
56. L. Kong, M. Huang, J. Chen, M. Lin, Fabrication of sensitive silver-decorated cotton swabs for SERS quantitative detection of mixed pesticide residues in bitter gourds. New J. Chem. **44**(29), 12779–12784 (2020). https://doi.org/10.1039/D0NJ02054K
57. P. Wu, L. Bin Zhong, Q. Liu, X. Zhou, Y.M. Zheng, Polymer induced one-step interfacial self-assembly method for the fabrication of flexible, robust and free-standing SERS substrates for rapid on-site detection of pesticide residues. Nanoscale **11**(27), 12829–12836 (2019). https://doi.org/10.1039/c9nr02851j
58. J. Chen, M. Huang, L. Kong, M. Lin, Jellylike flexible nanocellulose SERS substrate for rapid in-situ non-invasive pesticide detection in fruits/vegetables. Carbohydr. Polym. **205**, 596–600 (2019). https://doi.org/10.1016/j.carbpol.2018.10.059
59. X. Gong, M. Tang, Z. Gong, Z. Qiu, D. Wang, M. Fan, Screening pesticide residues on fruit peels using portable Raman spectrometer combined with adhesive tape sampling. Food Chem. **295**, 254–258 (2019). https://doi.org/10.1016/j.foodchem.2019.05.127
60. L. Jiang, K. Gu, R. Liu, S. Jin, H. Wang, C. Pan, Rapid detection of pesticide residues in fruits by surface-enhanced Raman scattering based on modified QuEChERS pretreatment method with portable Raman instrument. SN Appl. Sci. **1**(6), 627 (2019). https://doi.org/10.1007/s42452-019-0619-9
61. G. Kwon, J. Kim, D. Kim, Y. Ko, Y. Yamauchi, J. You, Nanoporous cellulose paper-based SERS platform for multiplex detection of hazardous pesticides. Cellulose **26**(8), 4935–4944 (2019). https://doi.org/10.1007/s10570-019-02427-8
62. L. Tognaccini, M. Ricci, C. Gellini, A. Feis, G. Smulevich, M. Becucci, Surface enhanced raman spectroscopy for in-field detection of pesticides: a test on dimethoate residues in water and on olive leaves. Molecules **24**(2) (2019). https://doi.org/10.3390/molecules24020292
63. L. Bin Zhong, Q. Liu, P. Wu, Q.F. Niu, H. Zhang, Y.M. Zheng, Facile on-site aqueous pollutant monitoring using a flexible, ultralight, and robust surface-enhanced Raman spectroscopy substrate: interface self-assembly of Au@Ag nanocubes on a polyvinyl chloride template. Environ. Sci. Technol. **52**(10), 5812–5820 (2018). https://doi.org/10.1021/acs.est.7b04327
64. H. Dies, M. Siampani, C. Escobedo, A. Docoslis, Direct detection of toxic contaminants in minimally processed food products using dendritic surface-enhanced Raman scattering substrates. Sensors **18**(8), 2726 (2018). https://doi.org/10.3390/s18082726
65. J. Hong, A. Kawashima, N. Hamada, A simple fabrication of plasmonic surface-enhanced Raman scattering (SERS) substrate for pesticide analysis via the immobilization of gold nanoparticles on UF membrane. Appl. Surf. Sci. **407**, 440–446 (2017). https://doi.org/10.1016/j.apsusc.2017.02.232
66. K. Wang et al., A 'drop-wipe-test' SERS method for rapid detection of pesticide residues in fruits. J. Raman Spectrosc. **49**(3), 493–498 (2018). https://doi.org/10.1002/jrs.5308
67. Q. Xu et al., Template-free synthesis of SERS-active gold nanopopcorn for rapid detection of chlorpyrifos residues. Sensors Actuators, B Chem. **241**, 1008–1013 (2017). https://doi.org/10.1016/j.snb.2016.11.021
68. A. González Fá, F. Pignanelli, I. López-Corral, R. Faccio, A. Juan, M.S. Di Nezio, Detection of oxytetracycline in honey using SERS on silver nanoparticles. TrAC Trends Anal. Chem. **121**, 115673 (2019). https://doi.org/10.1016/j.trac.2019.115673
69. M. Li et al., Heterostructured cube Au-Ag composites for rapid Raman detection of antibiotic ciprofloxacin. J. Raman Spectrosc. **48**(4), 525–529 (2017). https://doi.org/10.1002/jrs.5071
70. M. Sourdaine et al., Protecting the food supply chain: Utilizing SERS and portable Raman spectroscopy. Tech. Mess. **82**(12), 625–632 (2015). https://doi.org/10.1515/teme-2015-0046
71. L. Ouyang, L. Zhu, Y. Ruan, H. Tang, Preparation of a native β-cyclodextrin modified plasmonic hydrogel substrate and its use as a surface-enhanced Raman scattering scaffold for antibiotics identification. J. Mater. Chem. C **3**(29), 7575–7582 (2015). https://doi.org/10.1039/C5TC01368B
72. W. Cao et al., Detection of benzo[a]pyrene with silver nanorod substrate in river water and soil based on surface-enhanced raman scattering. Results Chem. **3**, 100126 (2021). https://doi.org/10.1016/j.rechem.2021.100126
73. X. Huang et al., Controllable self-assembled plasmonic vesicle-based three-dimensional SERS platform for picomolar detection of hydrophobic contaminants. Nanoscale **10**(27), 13202–13211 (2018). https://doi.org/10.1039/C8NR02778A
74. F. Zeng et al., Paper-based versatile surface-enhanced Raman spectroscopy chip with smartphone-based Raman analyzer for point-of-care application. Anal. Chem. **91**(1), 1064–1070 (2019). https://doi.org/10.1021/acs.analchem.8b04441
75. J. Liu et al., CRISPR-/Cas12a-mediated liposome-amplified strategy for the surface-enhanced Raman scattering and naked-eye detection of nucleic acid and application to food authenticity screening. Anal. Chem. **93**(29), 10167–10174 (2021). https://doi.org/10.1021/acs.analchem.1c01163
76. P. Zhang et al., Rapid detection of 6-Benzylaminopurine residuals using surface-enhanced Raman scattering. J. Appl.

Spectrosc. **85**(5), 880–884 (2018). https://doi.org/10.1007/s10812-018-0733-2
77. D. Li et al., Chromatographic separation and detection of contaminants from whole milk powder using a chitosan-modified silver nanoparticles surface-enhanced Raman scattering device. Food Chem. **224**, 382–389 (2017). https://doi.org/10.1016/j.foodchem.2016.12.040
78. S. Lin et al., Lab-on-capillary platform for on-site quantitative SERS analysis of surface contaminants based on Au@4-MBA@Ag core–shell nanorods. ACS Sensors **5**(5), 1465–1473 (2020). https://doi.org/10.1021/acssensors.0c00398
79. M. Sun et al., Performance enhancement of paper-based SERS chips by shell-isolated nanoparticle-enhanced Raman spectroscopy. J. Mater. Sci. Technol. **35**(10), 2207–2212 (2019). https://doi.org/10.1016/j.jmst.2019.05.055
80. G. Brackx et al., A frugal implementation of surface enhanced Raman scattering for sensing Zn2+ in freshwaters – in depth investigation of the analytical performances. Sci. Rep. **10**(1), 1883 (2020). https://doi.org/10.1038/s41598-020-58647-7
81. C. Wang et al., Specific and sensitive on-site detection of Cr(VI) by surface-enhanced Raman spectroscopy. Sensors Actuators B Chem. **346**, 130594 (2021). https://doi.org/10.1016/j.snb.2021.130594
82. J. Pretty, Agricultural sustainability: concepts, principles and evidence. Philos. Trans. R. Soc. B Biol. Sci. **363**(1491), 447–465 (2008). https://doi.org/10.1098/rstb.2007.2163
83. P. Nicolopoulou-Stamati, S. Maipas, C. Kotampasi, P. Stamatis, L. Hens, Chemical Pesticides and human health: the urgent need for a new concept in agriculture. Front. Public Heal. **4**, 148 (2016). https://doi.org/10.3389/FPUBH.2016.00148/BIBTEX
84. S. Pang, T. Yang, L. He, Review of surface enhanced Raman spectroscopic (SERS) detection of synthetic chemical pesticides. TrAC Trends Anal. Chem. **85**, 73–82 (2016). https://doi.org/10.1016/j.trac.2016.06.017
85. A.M. Dowgiallo, D.A. Guenther, Determination of the limit of detection of multiple pesticides utilizing gold nanoparticles and surface-enhanced Raman spectroscopy. J. Agric. Food Chem. **67**(46), 12642–12651 (2019). https://doi.org/10.1021/acs.jafc.9b01544
86. B. Liu et al., Shell thickness-dependent Raman enhancement for rapid identification and detection of pesticide residues at fruit peels. Anal. Chem. **84**(1), 255–261 (2012). https://doi.org/10.1021/ac202452t
87. J. Jiang, S. Zou, L. Ma, S. Wang, J. Liao, Z. Zhang, Surface-enhanced Raman scattering detection of pesticide residues using transparent adhesive tapes and coated silver nanorods. ACS Appl. Mater. Interfaces **10**(10), 9129–9135 (2018). https://doi.org/10.1021/acsami.7b18039
88. O. Guselnikova, V. Svorcik, O. Lyutakov, M.M. Chehimi, P.S. Postnikov, Preparation of selective and reproducible SERS sensors of Hg2+ ions via a sunlight-induced thiol–Yne reaction on gold gratings. Sensors **19**(9), 2110 (2019). https://doi.org/10.3390/s19092110
89. Y. Wu, Y. Liu, X. Tang, Z. Cheng, H. Liu, Tunable plasmonics of hollow raspberry-like nanogold for the robust Raman scattering detection of antibiotics on a portable Raman spectrometer. Analyst **145**(17), 5854–5860 (2020). https://doi.org/10.1039/d0an01049a
90. Q. Shi et al., A SERS-based multiple immuno-nanoprobe for ultrasensitive detection of neomycin and quinolone antibiotics via a lateral flow assay. Microchim. Acta **185**(2), 3–10 (2018). https://doi.org/10.1007/s00604-017-2556-x
91. World Health Organization, UN strengthens regulations on melamine, seafood, melons, dried figs and labelling, Saudi medical journal, vol. 33, no. 8. World Health Organization, pp. 920–921 (2012), Accessed: Dec. 17, 2021. [Online]. Available: https://www.who.int/news/item/04-07-2012-un-strengthens-regulations-on-melamine-seafood-melons-dried-figs-and-labelling
92. World Health Organisation, Toxicological and health aspects of melamine and cyanuric acid, World Health Organisation, (2009). https://apps.who.int/iris/bitstream/handle/10665/44106/9789241597951_eng.pdf?sequence=1 (accessed Dec. 17, 2021)
93. C.A. Brown et al., Outbreaks of renal failure associated with melamine and cyanuric acid in dogs and cats in 2004 and 2007. J. Vet. Diagnostic Investig. **19**(5), 525–531 (2007). https://doi.org/10.1177/104063870701900510
94. H. Wu et al., A simple SERS-based trace sensing platform enabled by AuNPs-Analyte/AuNPs double-decker structure on wax-coated hydrophobic surface. Front. Chem. **6**, 1–9 (2018). https://doi.org/10.3389/fchem.2018.00482
95. J. Raveendran, A. Docoslis, Portable surface-enhanced Raman scattering analysis performed with microelectrode-templated silver nanodendrites. Analyst **145**(13), 4467–4476 (2020). https://doi.org/10.1039/D0AN00484G
96. K. Ge, Y. Hu, Y. Zheng, P. Jiang, G. Li, Aptamer/derivatization-based surface-enhanced Raman scattering membrane assembly for selective analysis of melamine and formaldehyde in migration of melamine kitchenware. Talanta **235**, 122743 (2021). https://doi.org/10.1016/j.talanta.2021.122743
97. F. Fang, Y. Qi, F. Lu, L. Yang, Highly sensitive on-site detection of drugs adulterated in botanical dietary supplements using thin layer chromatography combined with dynamic surface enhanced Raman spectroscopy. Talanta **146**, 351–357 (2016). https://doi.org/10.1016/j.talanta.2015.08.067
98. X. Guo, D. Wang, R. Khan, Nafion stabilized Ag nanopillar arrays as a flexible SERS substrate for trace chemical detection. Mater. Chem. Phys. **252**, 123291 (2020). https://doi.org/10.1016/j.matchemphys.2020.123291
99. L. Kong, J. Chen, M. Huang, GO/Au@Ag nanobones decorated membrane for simultaneous enrichment and on-site SERS detection of colorants in beverages. Sensors Actuators B Chem. **344**, 130163 (2021). https://doi.org/10.1016/j.snb.2021.130163
100. L. Lebreton, M. Egger, B. Slat, A global mass budget for positively buoyant macroplastic debris in the ocean. Sci. Rep. **9**(1), 12922 (2019). https://doi.org/10.1038/s41598-019-49413-5
101. Plastics Europe, Plastics Europe • enabling a sustainable future, Plastics Europe, (2021). https://plasticseurope.org/ (accessed Nov. 29, 2021)
102. J.R. Jambeck, R. Geyer, C. Wilcox, T.R. Siegler, M. Perryman, A. Andrady, R. Narayan, K.L. Law, Plastic waste inputs from land into the ocean. Science **347**(6223), 768–771 (2015). https://doi.org/10.1126/science.1260352
103. Y. Tang et al., A review: research progress on microplastic pollutants in aquatic environments. Sci. Total Environ. **766**, 142572 (2021). https://doi.org/10.1016/j.scitotenv.2020.142572
104. M. Pivokonsky, L. Cermakova, K. Novotna, P. Peer, T. Cajthaml, V. Janda, Occurrence of microplastics in raw and treated drinking water. Sci. Total Environ. **643**, 1644–1651 (2018). https://doi.org/10.1016/j.scitotenv.2018.08.102
105. C. Campanale et al., Microplastics and their possible sources: the example of Ofanto river in southeast Italy. Environ. Pollut. **258**, 113284 (2020). https://doi.org/10.1016/j.envpol.2019.113284
106. J.C. Prata, Airborne microplastics: consequences to human health? Environ. Pollut. **234**, 115–126 (2018). https://doi.org/10.1016/j.envpol.2017.11.043
107. M. Campanale, Savino, Locaputo, and Uricchio, A detailed review study on potential effects of microplastics and additives of concern on human health. Int. J. Environ. Res. Public Health **17**(4), 1212 (2020). https://doi.org/10.3390/ijerph17041212
108. S.L. Wright, F.J. Kelly, Plastic and Human health: a micro issue? Environ. Sci. Technol. **51**(12), 6634–6647 (2017). https://doi.org/10.1021/ACS.EST.7B00423/SUPPL_FILE/ES7B00423_SI_001.PDF

109. J.S. Silva-Cavalcanti, J.D.B. Silva, E.J. de França, M.C.B. de Araújo, F. Gusmão, Microplastics ingestion by a common tropical freshwater fishing resource. Environ. Pollut. **221**, 218–226 (2017). https://doi.org/10.1016/j.envpol.2016.11.068
110. J. Gasperi et al., Microplastics in air: are we breathing it in? Curr. Opin. Environ. Sci. Heal. **1**, 1–5 (2018). https://doi.org/10.1016/j.coesh.2017.10.002
111. M. Revel, A. Châtel, C. Mouneyrac, Micro(nano)plastics: a threat to human health? Curr. Opin. Environ. Sci. Heal. **1**, 17–23 (2018). https://doi.org/10.1016/j.coesh.2017.10.003
112. G.F. Schirinzi, I. Pérez-Pomeda, J. Sanchís, C. Rossini, M. Farré, D. Barceló, Cytotoxic effects of commonly used nanomaterials and microplastics on cerebral and epithelial human cells. Environ. Res. **159**, 579–587 (2017). https://doi.org/10.1016/j.envres.2017.08.043
113. D.M. Monti et al., Biocompatibility, uptake and endocytosis pathways of polystyrene nanoparticles in primary human renal epithelial cells. J. Biotechnol. **193**, 3–10 (2015). https://doi.org/10.1016/j.jbiotec.2014.11.004
114. K.D. Cox, G.A. Covernton, H.L. Davies, J.F. Dower, F. Juanes, S.E. Dudas, Human consumption of microplastics. Environ. Sci. Technol. **53**(12), 7068–7074 (2019). https://doi.org/10.1021/acs.est.9b01517
115. P. Schwabl et al., Detection of various microplastics in human stool: a prospective case series. Ann. Intern. Med. **171**(7), 453–457 (2019). https://doi.org/10.7326/M19-0618
116. A. Vianello, R. L. Jensen, L. Liu, J. Vollertsen, Simulating human exposure to indoor airborne microplastics using a Breathing Thermal Manikin. Sci. Reports 91, 9 (1), 1–11, (2019). https://doi.org/10.1038/s41598-019-45054-w
117. M. Xu et al., Internalization and toxicity: a preliminary study of effects of nanoplastic particles on human lung epithelial cell. Sci. Total Environ. **694**, 133794 (2019). https://doi.org/10.1016/j.scitotenv.2019.133794
118. A.H. Iri et al., Optical detection of microplastics in water. Environ. Sci. Pollut. Res. **28**(45), 63860–63866 (2021). https://doi.org/10.1007/s11356-021-12358-2
119. L. Lv et al., In situ surface-enhanced Raman spectroscopy for detecting microplastics and nanoplastics in aquatic environments. Sci. Total Environ. **728**, 138449 (2020). https://doi.org/10.1016/j.scitotenv.2020.138449
120. R. Yin et al., Sensitive and rapid detection of trace microplastics concentrated through Au-nanoparticle-decorated sponge on the basis of surface-enhanced Raman spectroscopy. Environ. Adv. **5**, 100096 (2021). https://doi.org/10.1016/j.envadv.2021.100096
121. S.W.P. Wijnhoven et al., Nano-silver – a review of available data and knowledge gaps in human and environmental risk assessment. Nanotoxicology **3**(2), 109–138 (2009). https://doi.org/10.1080/17435390902725914
122. M.E. Quadros, L.C. Marr, Environmental and human health risks of aerosolized silver nanoparticles. J. Air Waste Manag. Assoc. **60**(7), 770–781 (2010). https://doi.org/10.3155/1047-3289.60.7.770
123. US EPA, Environmental Protection Agency. National Ambient Air Quality Standards (NAAQS) for PM, US EPA, (2020). https://www.epa.gov/pm-pollution/national-ambient-air-quality-standards-naaqs-pm (accessed Dec. 22, 2021)
124. H. Guo et al., Analysis of silver nanoparticles in antimicrobial products using Surface-Enhanced Raman Spectroscopy (SERS). Environ. Sci. Technol. **49**(7), 4317–4324 (2015). https://doi.org/10.1021/acs.est.5b00370
125. H. Guo, B. Xing, L. He, Development of a filter-based method for detecting silver nanoparticles and their heteroaggregation in aqueous environments by surface-enhanced Raman spectroscopy. Environ. Pollut. **211**, 198–205 (2016). https://doi.org/10.1016/j.envpol.2015.12.049
126. M. Quarato, I. Pinheiro, A. Vieira, B. Espiña, and L. Rodriguez-Lorenzo, Detection of silver nanoparticles in seawater using surface-enhanced raman scattering. Nanomaterials **11**(7) (2021). https://doi.org/10.3390/nano11071711
127. H. Guo, B. Xing, J.C. White, A. Mukherjee, L. He, Ultra-sensitive determination of silver nanoparticles by surface-enhanced Raman spectroscopy (SERS) after hydrophobization-mediated extraction. Analyst **141**(18), 5261–5264 (2016). https://doi.org/10.1039/C6AN01186A
128. G. Xu et al., Surface-enhanced Raman spectroscopy facilitates the detection of microplastics <1 μm in the environment. Environ. Sci. Technol. **54**(24), 15594–15603 (2020). https://doi.org/10.1021/acs.est.0c02317
129. X.X. Zhou, R. Liu, L.T. Hao, J.F. Liu, Identification of polystyrene nanoplastics using surface enhanced Raman spectroscopy. Talanta **221**, 121552 (2021). https://doi.org/10.1016/j.talanta.2020.121552
130. Q.T. Lê et al., Nanostructured Raman substrates for the sensitive detection of submicrometer-sized plastic pollutants in water. J. Hazard. Mater. **402**, 123499 (2021). https://doi.org/10.1016/j.jhazmat.2020.123499
131. J. Caldwell, P. Taladriz-Blanco, B. Rothen-Rutishauser, A. Petri-Fink, Detection of sub-micro- and nanoplastic particles on gold nanoparticle-based substrates through Surface-Enhanced Raman Scattering (SERS) Spectroscopy. Nanomaterials **11**(5), 1149 (2021). https://doi.org/10.3390/nano11051149
132. Y. Jeon et al., Detection of nanoplastics based on surface-enhanced Raman scattering with silver nanowire arrays on regenerated cellulose films. Carbohydr. Polym. **272**, 118470 (2021). https://doi.org/10.1016/j.carbpol.2021.118470